Exact solution of the t-J model in one dimension at $2t = \pm J$: Ground state and excitation spectrum

P.-A. Bares, G. Blatter, and M. Ogata
Theoretische Physik, ETH-Hönggerberg, 8093 Zürich, Switzerland
(Received 2 January 1991)

The one dimensional t-J Hamiltonian is diagonalized exactly for the supersymmetric case $2t = \pm J$ using the Bethe ansatz. In this limit it is identical with models previously considered by Lai, Sutherland, and Schlottmann. In the present paper we discuss the ground-state properties and excitation spectrum in zero magnetic field. The ground state is a liquid of singlet bonds with varying spatial separation. Its most remarkable feature is the presence of bonds connecting particles at arbitrarily large distances. The ground-state energy is an analytic function of the band filling. There is no difference in the chemical potential for adding one or two particles and no evidence for the binding of holes. The low-lying part of the spectrum consists of two types of gapless excitations (charge and spin) with effective Fermi surfaces at $2k_F$ and k_F, respectively. An interpretation of the energy spectrum in terms of spinons and holons is appropriate at low energies.

I. INTRODUCTION

Strongly correlated systems are of current interest in view of their relevance to the theory of high-T_c superconductivity. In particular, Anderson has suggested that the t-J model is an appropriate starting model.[1,2] The model describes the behavior of hard core electrons on a discrete lattice: the dynamics is given by a Hamiltonian which includes nearest neighbor hopping (t) and antiferromagnetic exchange (J).

In one dimension, Lieb and Wu[3] diagonalized the Hubbard Hamiltonian, a closely related model. It is known that the large-U repulsive Hubbard model maps onto the limit $J \ll t$ of the t-J model.[4] Nevertheless, the t-J model can be studied in its own right as an independent model. In two dimensions many fundamental aspects of the model remain elusive. Recently, Anderson claimed[5] that 2D strongly correlated models may share features of the one-dimensional systems. It is instructive to study an exact solution in one dimension.

In this paper we focus attention on the one-dimensional t-J model and study the exact solution at $2t = J$. We emphasize that the model we discuss cannot be obtained as the large-U limit of the Hubbard model. The supersymmetric t-J model has two levels of strong correlation: an infinite on-site Coulomb repulsion and a large exchange interaction.

There has been previous work using the Bethe ansatz on one-dimensional models involving both hard core fermions and bosons. However, these investigations have been performed in a different context and it is only recently that their connection to the t-J model has been established. In 1974, Lai introduced a quantum lattice-gas model, which is identical (up to a term) with the t-J model.[6] He first applied the Bethe ansatz technique to diagonalize the Hamiltonian and discovered a solution at $2t = \pm J$ ($\Delta = \pm 1$ in Lai's notation). Shortly thereafter, Sutherland[7] showed Lai's results to be partly incorrect and derived the Bethe-ansatz equations for a general multicomponent lattice-gas model, including the case considered by Lai. In 1987, Schlottmann[8] discovered the solution at $2t = \pm J$ by means of the quantum inverse scattering method (QISM), presented the Bethe-ansatz equations for the ground state in a magnetic field and discussed the thermodynamic properties of the model, applying his results to heavy-fermion systems. Stimulated by the recent interest in strongly correlated systems, one of us examined the question of exact integrability in the t-J model and rediscovered the solution at $2t = \pm J$ (Ref. 9) in the form given by Lai and Schlottmann.[6,8] In Ref. 10 a summary of part of the results on the excitation spectrum of the model and a brief discussion of the mechanism of separation of charge and spin degrees of freedom have been presented. Also, Sarkar[11] reproduced Sutherland's form of the solution by applying the Bethe ansatz to the t-J Hamiltonian.[12]

A series of numerical calculations on finite clusters has been performed by Imada *et al.*,[13] by Von Szczepanski *et al.*,[14] and, using quantum Monte Carlo techniques, by Assaad and Würtz.[15] Very recently, the phase diagram of the one-dimensional t-J model has been studied numerically.[16] These numerical studies show clearly that the t-J model belongs to the same universality class as that of the repulsive Hubbard model: The t-J model is a Luttinger liquid in the sense of Haldane.[17] By applying finite-size analysis in conformal field theory,[18,19] Kawakami and Yang[20] calculated the exponents of the large distance behavior of charge, spin, and superconducting correlation functions, and the zero temperature specific heat and magnetic susceptibility. Alternatively, the latter thermodynamic properties can be derived by a method due to Carmelo and Ovchinnikov.[21,22] Their "Landau-Luttinger-liquid" formulation of the Bethe-ansatz equations permits a direct determination of the interaction between the spinons and holons. These interaction functions can be expressed in terms of scattering phase shifts

and spinon (holon) velocities:[21–25] They are related to the "dressed charge matrix" of conformal field theory.[19,18]

In the present work we investigate in detail the ground state and excitation spectrum of the supersymmetric t-J model. The ground state is a liquid of singlet bonds connecting spins at arbitrary large distances. The excitation spectrum reveals unusual and interesting features. The holon-antiholon (charge) spectrum shows an apparent gap in momentum space above the band filling $n=\frac{2}{3}$. There exist charge excitations at $\pm 2k_F (k_F=\pi n/2)$ which however are composite and involve the emission of pairs of antiparallel FM domain walls (spinons). At very low energies, the spin excitation spectrum can be interpreted as a spinon spectrum over a wide range of filling. However, in the dilute limit, the spin excitation spectrum transforms into a particle spectrum where charge and spin have recombined. Careful investigations of the excitation spectrum of even and odd chains near half-filling lead us to surprising results. The pure spinon spectrum in an odd chain extends over a restricted region of the Brillouin zone. However, there are composite excitations which have as the lowest branch a spinonlike spectrum in the complementary region of momentum space. The propagation of the spinon in this region of the Brillouin zone is characterized by the emission of spinon pairs in a singlet state. Also the holon spectrum of the t-J model in an odd chain is seen to have a $2k_F$ periodicity in contrast with that of the Hubbard model, which is $4k_F$ periodic. A physical picture of this unusual situation is proposed. Upon doping an even chain with one hole, the separation of the charge and spin degrees of freedom occurs at very low energies: the one-hole spectrum is two parametric and is given additively by the spinon (spin) and holon (charge) contributions. Furthermore, the supersymmetric properties of the t-J model show up in finite chains as specific relations between the energy eigenvalues of systems differing by one or two particles.

The plan of the paper is a follows. Section II is devoted to the diagonalization of the t-J Hamiltonian by means of the algebraic Bethe ansatz (QISM). At $2t=\pm J$, the eigenvalue problem can be reduced to that of diagonalizing the transfer matrix of a six-vertex model, the general solution of which is well known.[26–31] In Ref. 25 we consider the eigenvalue problem in the framework of the coordinate Bethe ansatz and reduce the problem to a form which is essentially identical with Yang's solution of the fermion gas with a δ-function repulsive potential.[26] The problem of constructing the spectrum is transformed in a standard way into that of solving a set of coupled algebraic equations, the so-called "Bethe-ansatz equations" (BAE). We derive the BAE in the form first given by Lai[6] and discuss briefly the solution due to Sutherland.[7] In Sec. III we present the solution of the BAE for the ground state in Lai's formulation. In Sec. IV we deal with the excitation spectrum and find gapless charge and spin excitations. The charge spectrum is identified as the holon-antiholon spectrum and, at low energies, the spin spectrum as the spinon spectrum. In Sec. V we establish the connection between Lai's form (complex roots for the ground state) of the BAE and that of Sutherland (real roots for the ground state). We then reproduce in Sutherland's formulation the results of the previous sections. In Sec. VI we consider the problem of a few holes in a half-filled band, study the separation of charge and spin degrees of freedom, and discuss the spinon and holon spectra in odd chains. Section VII contains a brief discussion of the supersymmetry in the model.

Our purpose is a comprehensive and simple presentation of the results and so we omit lengthy algebra. The interested reader may find the details in Ref. 25.

II. THE MODEL AND ITS BASIC EQUATIONS AT $2t=\pm J$

A one-dimensional lattice of N_a sites (unit lattice constant) with N electrons is considered. We assume each site is capable of accommodating at most one particle, and the dynamics of the hard core fermions is described by the Hamiltonian

$$H_{tJ}=\mathcal{P}\left[-t\sum_{\langle i,j\rangle\sigma}(c_{i\sigma}^{\dagger}c_{j\sigma}+\text{H.c.})+J\sum_{\langle i,j\rangle}\left[\mathbf{S}_i\cdot\mathbf{S}_j-\frac{n_i\cdot n_j}{4}\right]\right]\mathcal{P}\,, \tag{2.1}$$

where $\sum_{\langle i,j\rangle}$ is restricted to nearest-neighbor sites and $c_{i\sigma}^{\dagger}$ creates an electron of spin σ in a Wannier state at site i. $\mathbf{S}_j$ and $n_j=\sum_\sigma n_{j\sigma}(n_{j\sigma}=c_{j\sigma}^{\dagger}c_{j\sigma})$ are the usual spin and number operators, respectively. The projector $\mathcal{P}=\prod_{j=1}^{N_a}(1-n_{j\uparrow}n_{j\downarrow})$ has been included to ensure the constraint of no double occupancy. Notice that the convention for J adopted in the present paper differs by a factor 2 from that of Ref. 10. The Hamiltonian H_{tJ} acts on a projected Hilbert space $\mathcal{H}_N$ of dimension $2^N\binom{N_a}{N}$, containing N-particle states with no doubly occupied sites. We seek eigenstates in the form

$$|\Psi\rangle=\sum_x\psi(x_1,\sigma_1;\cdots;x_N,\sigma_N)\prod_j^N c_{x_j\sigma_j}^{\dagger}|0\rangle\,, \tag{2.2a}$$

where $\sum_x$ means that the sum is carried out over the appropriate space labels. The fermion operators $c_{j,\sigma}^{(\dagger)}$ cannot be used in treating particles with hard core, since the projective transformation on the Hilbert space alters the canonical commutation relations. For our purposes, it is more convenient to retain the fermion field operators and to impose the subsidiary condition on the allowable state vectors (2.2a):

$$\psi(\ldots;x,\sigma_i;\ldots;x,\sigma_j;\ldots)=0\,. \tag{2.2b}$$

The reason for retaining the projector in Eq. (2.1) is a technical one. Below we introduce amplitudes Ψ which coincide with the physical amplitudes ψ if the space coordinates of the particles are all different, but do not if two space labels are equal. The point is that a Bethe ansatz for Ψ does not allow us to set $\Psi=0$ whenever $x_i=x_j$. However, it can be shown that our method of solution[32] is equivalent to that of solving the eigenvalue problem directly for the physical amplitudes ψ.[25] Therefore, within the framework of the Bethe ansatz, the constraint

of no double occupancy is treated in an exact way. In one dimension the exact solution of the t-J model may be used to check the validity of the approximation schemes developed to treat the local constraint of no double occupancy (slave boson or fermion techniques).

In order to enumerate a complete set of eigenstates, one usually imposes periodic boundary conditions (PBC):[33]

$$\Psi(\ldots;x_j,\sigma_j;\ldots)=\Psi(\ldots;x_j+N_a,\sigma_j;\cdots)\ . \tag{2.2c}$$

Our task is to diagonalize H_{tJ} subject to the PBC (2.2c) using the Bethe ansatz.[34] The method devised by Bethe has been reformulated and generalized by a number of authors.[26–31] We apply here the algebraic Bethe ansatz or quantum inverse scattering method (QISM).[29,30] A derivation of the same results in terms of the old coordinate Bethe ansatz is given in Ref. 25.

In the first place let us review some basic facts. The fundamental region[35] of the phase plane is sketched in Fig. 1. On the line AB the t-J model is equivalent to a free spinless-fermion system, whereas on the line BC the model reduces to the Heisenberg chain. The line AC denotes the singlet sector. The complementary region can be obtained by symmetry. D is a point of high symmetry and so a good candidate for a singular point.

The t-J Hamiltonian is U(1)-gauge and SU(2)-spin invariant. In addition, the model becomes supersymmetric at $2t=\pm J$ (see Sec. VI).[36,37] The spectrum of H_{tJ} is invariant under a unitary transformation which changes the sign of t^3 and the spectrum of $H_{tJ}(-J)$ is that of $H_{tJ}(J)$ inverted.[38] For definiteness, we assume $t>0$ in (2.1) and study in this work the antiferromagnetic case (AFM).

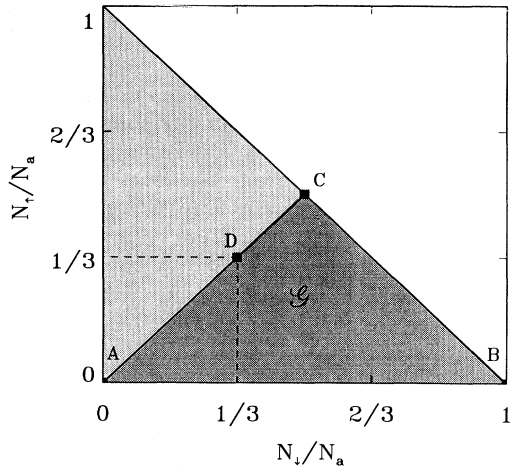

FIG. 1. Phase plane for the one-dimensional t-J model: $\mathcal{G}$ denotes the fundamental region for which the Bethe ansatz is a solution. The physical properties of the model are analytic in $\mathcal{G}$. The point A marks the dilute limit which behaves free electron-like, B denotes the ferromagnetic state, and C is the antiferromagnetic ground state at half-filling. D is a point of high symmetry where the number of down spins, up spins, and holes are equal.

In the first quantized representation, the eigenvalue problem reads

$$-t\sum_{j,s}^{N}\left[1-\sum_{i=1}^{N}\delta_{x_i+s,x_j}\delta_{-\sigma_i,\sigma_j}\right]\Psi(\ldots;x_j+s,\sigma_j;\ldots)$$
$$+\frac{J}{2}\sum_{i<j,s}\delta_{x_i+s,x_j}\delta_{-\sigma_i,\sigma_j}(\mathcal{P}_\sigma^{ij}-1)\Psi(\ldots;x_i,\sigma_i;\ldots;x_j,\sigma_j;\ldots)=E\Psi(x_1,\sigma_1;\ldots;x_N,\sigma_N)\ , \tag{2.3}$$

where $\mathcal{P}_\sigma^{ij}=\frac{1}{2}(1+\boldsymbol{\sigma}_i\cdot\boldsymbol{\sigma}_j)$.

To construct eigenstates it is convenient to divide configuration space into $N!$ regions, R_Q, labeled by the permutation Q according to the ordering of the particles on the lattice: $x_{Q_1}<x_{Q_2}<\cdots<x_{Q_N}$. Consider the case when all the particles are well separated. In the interior of region R_Q, the wave function is of the Bethe-ansatz form

$$\Psi(x_1\sigma_1;\cdots;x_N\sigma_N)=\sum_{P\in\Pi_N}(-1)^P A_{\sigma_{Q_1}\cdots\sigma_{Q_N}}(PQ)\exp\left[i\sum_j k_{P_j}x_j\right]\ . \tag{2.4}$$

P,Q denote permutations of the numbers $1,\ldots,N$; $(-1)^P$ is the sign of the permutation P and guarantees the antisymmetry of the amplitude under permutation of identical particles. The energy and the momentum of the eigenfunction (2.4) are given, respectively, by

$$E=-2t\sum_{j=1}^{N}\cos k_j\ , \tag{2.5a}$$

$$P=\sum_{j=1}^{N}k_j\ . \tag{2.5b}$$

Let us now turn to the actual problem of interacting particles and rewrite Eq. (2.3) as

$$-t\sum_{j,s=\pm1}\Psi(\ldots;x_j+s,\sigma_j;\cdots)+\sum_{i<j,s}\delta_{x_i+s,x_j}\delta_{-\sigma_i,\sigma_j}\{t[\Psi(\ldots;x_i+s,\sigma_i;\ldots;x_j,\sigma_j;\ldots)$$
$$+\Psi(\ldots;x_i,\sigma_i;\ldots;x_j-s,\sigma_j;\ldots)]+\frac{J}{2}(\mathcal{P}_\sigma^{ij}-1)\Psi(\ldots;x_i,\sigma_i;\ldots;x_j,\sigma_j;\ldots)\} \tag{2.6}$$

Notice that the symbol $\delta_{-\sigma_i\sigma_j}$ in front of the second term on the left-hand side (LHS) of Eq. (2.6) is not necessary, due to the antisymmetry of Ψ.

In order for Ψ to be an eigenfunction, the term in curly brackets on the LHS of (2.6) must vanish. For this purpose we extend the form (2.4) of the amplitudes in configuration space so as to include the boundaries of the sectors R_Q. At the boundaries of R_Q, amplitudes with equal space labels arise: these amplitudes are dummy since they have no physical meaning. This leads us to the core of the strategy: by a *judicious choice of the dummy amplitudes* one is able to cancel the terms generated by the interaction in (2.6). This condition establishes a set of linear equations between the coefficients $A_{\sigma_{Q1}\cdots\sigma_{QN}}(PQ)$ defined in different regions of configuration space. The linear relations between the coefficients $A_{\sigma_{Q1}\cdots\sigma_{QN}}(PQ)$ define a multiparticle S matrix

$$A_{\sigma_{Q1}\cdots\sigma_{QN}}(PQ')=(S_{ij})^{\sigma_{Q1'}\cdots\sigma_{QN'}}_{\sigma_{Q1}\cdots\sigma_{QN}}A_{\sigma_{Q1'}\cdots\sigma_{QN'}}(PQ)\ , \tag{2.7a}$$

where summation over repeated indices is meant and $Q'=Q(ll+1)$, with (ij) denoting the transposition of i and j. In (2.7a) the multiparticle S matrix is given by

$$(S_{ij})^{\sigma_1'\cdots\sigma_N'}_{\sigma_1\cdots\sigma_N}=(S(k,k'))^{\sigma_i\sigma_i'}_{\sigma_j\sigma_j'}\prod_{l\neq i,j}\delta_{\sigma_l\sigma_l'}\ , \tag{2.7b}$$

with the two-particle scattering matrix defined by

$$(S(k,k'))^{\sigma_i\sigma_i'}_{\sigma_j\sigma_j'}=y_{kk'}^{-1}\delta_{\sigma_i\sigma_i'}\delta_{\sigma_j\sigma_j'}+(1-y_{kk'}^{-1})\delta_{\sigma_i\sigma_j'}\delta_{\sigma_j\sigma_i'} \tag{2.7c}$$

and

$$y_{kk'}^{-1}=\frac{g(e^{ik}-e^{ik'})}{2ge^{ik}-(1+e^{(k+k')})},\quad g=J/2t\ . \tag{2.7d}$$

The consistency of the Bethe ansatz[39] requires the multiparticle S matrix to factorize into two-particle scattering matrices. The factorization conditions [Yang-Baxter equations, see, for example, (30)] read

$$S(k_1,k_2)^{\sigma_1\sigma_1'}_{\sigma_2\sigma_2'}S(k_1,k_3)^{\sigma_1'\sigma_1''}_{\sigma_3\sigma_3'}S(k_2,k_3)^{\sigma_2'\sigma_2''}_{\sigma_3'\sigma_3''}$$
$$=S(k_2,k_3)^{\sigma_2\sigma_2'}_{\sigma_3\sigma_3'}S(k_1,k_3)^{\sigma_1\sigma_1'}_{\sigma_3'\sigma_3''}S(k_1,k_2)^{\sigma_1'\sigma_1''}_{\sigma_2'\sigma_2''}\ . \tag{2.8}$$

Equation (2.8) is fulfilled provided $|g|=1$ [the shortest way to see this is to rewrite $y_{kk'}^{-1}$ as a function $f(h(k)-h(k'))$ where $h(k)$ depends only on the pseudomomentum of one of the colliding particles]. At this particular value of $|g|$, the two-particle S matrix takes the simple form[25]

$$S(k,k')^{\sigma_i\sigma_i'}_{\sigma_j\sigma_j'}=\frac{v(k)-v(k')}{v(k)-v(k')+ig}\delta_{\sigma_i\sigma_i'}\delta_{\sigma_j\sigma_j'}$$
$$+\frac{ig}{v(k)-v(k')+ig}\delta_{\sigma_i\sigma_j'}\delta_{\sigma_j\sigma_i'}\ , \tag{2.9}$$

where $v(k)=\frac{1}{2}\cot(k/2)$ for $g=1$ and $v(k)=\frac{1}{2}\tan(k/2)$ for $g=-1$. Clearly, the latter case can be obtained from the former by a shift of π in the Brillouin zone.

At this stage it is important to recognize the two-particle scattering matrix as the vertex-weight matrix of an inhomogeneous six-vertex model. The periodic boundary conditions (2.2) can be expressed in terms of the transfer matrix T_j of the corresponding classical two-dimensional lattice model:

$$T_jA(I)=e^{ik_jN_a}A(I)\ , \tag{2.10a}$$

where I denotes the identity in the permutation group and T_j is defined as

$$T_j=S_{j+1\,j}\cdots S_{Nj}S_{1j}\cdots S_{j-1\,j} \tag{2.10b}$$

with $S_{i,j}=S(k_i,k_j)$. The eigenvalue-problem (2.10a) is a matrix eigenvalue problem in a space of dimension 2^N for the SU(2) tensor $A_{\sigma_1\cdots\sigma_N}(I)$. From (2.8) it follows that $[T_j,T_i]=0$ for all j and i, so that the eigenvectors of T_j can be chosen independently of j. The diagonalization of T_j is achieved by a purely algebraic procedure, based on the algebra of monodromy matrices. For details the reader is referred to the literature.[26–31]

The eigenvalue problem reduces to the task of solving a set of $(N+M)$-coupled algebraic equations for N electron rapidities v_j and M spin rapidities Λ_α (M is the number of down spins):[25]

$$e^{ik_jN_a}=\prod_{\beta=1}^{M}\frac{v_j-\Lambda_\beta+i/2}{v_j-\Lambda_\beta-i/2}\ , \tag{2.11a}$$

$$\prod_{j=1}^{N}\frac{v_j-\Lambda_\alpha+i/2}{v_j-\Lambda_\alpha-i/2}=-\prod_{\beta=1}^{M}\frac{\Lambda_\beta-\Lambda_\alpha+i}{\Lambda_\beta-\Lambda_\alpha-i}\ , \tag{2.11b}$$

where $v_j=\frac{1}{2}\cot(k_j/2)$ for $2t=J$ and $v_j=\frac{1}{2}\tan(k_j/2)$ for $2t=-J$. The first set of Eqs. (2.11) represent the periodic boundary conditions: the right-hand side (RHS) of Eq. (2.11a) is the eigenvalue of the transfer matrix of the corresponding six-vertex model. Equation (2.11b) represents the necessary conditions for the "unwanted terms" in the generalized Bethe ansatz to vanish. The Bethe eigenvectors are the leading vectors with respect to the action of SU(2), i.e., $S=S^z=N/2-M$ (S is the total spin). The set of Eqs. (2.11) is typical of the six-vertex model (rational case) and so is identical to that occurring in the solution of Lieb and Wu[3] of the Hubbard model, except for the parametrization $v(k)$.

By applying the same strategy, it is possible to generalize to higher spins. The Bethe-ansatz equations consist of a hierarchy of $(2s+1)$-coupled set of algebraic equations.[7,25]

Equations (2.11) were obtained by Lai, and later by Schlottmann,[6,8,40] In 1975, Sutherland discovered an alternative way of solving the problem and applied his strategy to a multicomponent lattice gas model, which incorporates a generalization of the t-J model to an arbitrary number of fermion species.[7] Sutherland's idea is to place N_a particles of arbitrary statistics on a lattice of N_a sites and to generate the dynamics by permuting neighboring objects. We restrict our discussion to the case F^2B (two fermions and one boson) of Ref. 7 which corresponds to the (spin $\frac{1}{2}$) t-J model, more precisely ($t=1$):

$$H_S=\sum_{j=1}^{N_a}\mathcal{P}_{j,j+1}\ , \tag{2.12}$$

where $H_{tJ}=H_S-(N-N_h)$ and N,N_h are the number operators for particles and holes, respectively (in the t-J model). $\mathcal{P}_{j,j+1}$ denotes a graded[41] permutation operator. Sutherland's approach is to treat the holes and the down spins as dynamical objects in a background of up spins, i.e., to write amplitudes $\psi(X_1,\ldots,X_{M_1})$ for the $M_1=N_h+N_\downarrow$ objects. Clearly, a particle-hole transformation connects Sutherland's representation to that of Lai. He finds the solution in the form

$$e^{ik_\alpha N_a}=-\prod_{j=1}^{M_2}\frac{v_\alpha-w_j+i/2}{v_\alpha-w_j-i/2}\prod_{\beta=1}^{M_1}\frac{v_\alpha-v_\beta-i}{v_\alpha-v_\beta+i}\ , \tag{2.13a}$$

$$\prod_{\beta=1}^{M_1}\frac{w_j-v_\beta-i/2}{w_j-v_\beta+i/2}=1\ , \tag{2.13b}$$

where $v_\alpha=\frac{1}{2}\tan(k_\alpha/2)$, $\alpha=1,\ldots,M_1=N_h+N_\downarrow$, and $j=1,\ldots,M_2=N_h$. The w_j's are the hole rapidities and thus parametrize charge degrees of freedom, whereas the v_α involve both spin and charge degrees of freedom. The energy and momentum are given by

$$E_S=N_a-2M_i-2\sum_{\alpha=1}^{M_1}\cos k_\alpha\ , \tag{2.14}$$

$$P=\sum_{\alpha=1}^{M_1}k_\alpha\ . \tag{2.15}$$

A subtlety arises at this point in the definition (2.15) of the momentum as the generator of lattice translations. In particular, a constant must be added to the expression (2.15) depending on the number of sites, of particles and spin downs as confirmed by exact diagonalization of small clusters[42] (see discussion in Sec. V). In the case of an odd number of lattice sites, the RHS of (2.13) should be corrected by a factor (-1) (see Sec. VI).

III. THE GROUND STATE IN THE ANTIFERROMAGNETIC SECTOR ($J>0$)

In Sec. II the original eigenvalue problem has been reduced to that of solving the coupled set of algebraic equations (2.11). In the infinite volume limit (fixed $n=N/N_a$), the roots of (2.11) proliferate rapidly and it becomes difficult to determine the roots which parametrize the ground state. In Appendix A, it is shown that real roots of (2.11) lead to a high excited state, which is continuously connected to the ferromagnetic state at half-filling (its most peculiar feature is the nonanalyticity at the symmetric point $n=\frac{2}{3}$). On physical grounds we expect the system to lower its energy by forming bound states. The analysis of an explicit set of roots at small N and N_a suggests the structure of the solution in the ground state as confirmed by numerical studies: we make a "two-string" ansatz according to which the roots of (2.11) cluster into complex conjugate pairs in the v plane [see Fig. 2(a)][6,8]

$$v_{\alpha\pm}=v_\alpha\pm i/2+O(e^{-\varepsilon N_a})\ , \tag{3.1a}$$

with

$$v_\alpha=\Lambda_\alpha \tag{3.1b}$$

for $\alpha=1,\ldots,M=N/2$ (assuming N even). For a finite system the ansatz (3.1) does not cover all cases and singular roots of (2.11) must be treated separately. Taking the thermodynamic limit of the system of Eqs. (2.11) is then a subtle problem.[25] In Appendix B, we discuss this point and notice that the results obtained from (3.1) are correct as long as we measure the crystal momentum of the excitations with respect to the ground state.

The "bound states" parametrized by (3.1) correspond to the poles of the S matrix. The physical content of (3.1) can be expressed by saying that the ground state is a liquid of singlet bonds connecting pairs with arbitrary spatial separation (essentially Hulthen's picture[43] of the ground state of the AFM Heisenberg chain).

We define the bond length by $\xi(k)=[\mathrm{Im}(k)]^{-1}$. In terms of the electron rapidities, ξ is given by

$$\xi(v)=2[\ln(1+v^{-2})]^{-1}+O(e^{-\varepsilon N_a})\ . \tag{3.2}$$

Notice that, as $v\to\infty$, the bond length $\xi(v)$ diverges, i.e., bonds connecting pairs at arbitrarily large distances.

On substitution of (3.1) into (2.11), the set of Eqs. (2.11b) is fulfilled within exponential accuracy whereas (2.11a) reduces to (N even)

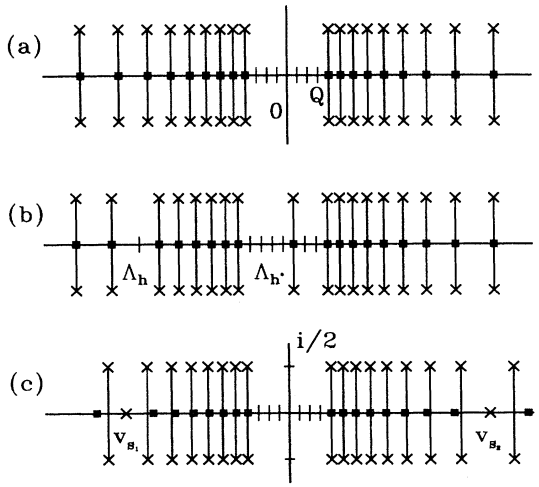

FIG. 2. Electron rapidities in the complex plane: Crosses ($\times$) denote the roots v_α describing kinetic degrees of freedom, filled squared ($\blacksquare$) denote the roots Λ_α associated with spin degrees of freedom. (a) Ground state: electron rapidities occur in complex pairs, $v_\alpha^\pm=v_\alpha\pm i/2$, describing singlet pairs of range $2/\ln(1+v_\alpha^{-2})$. The parameter Q determines the filling factor N/N_a. (b) Holon-antiholon (h-h^*) excitation: A string at v_h is transferred to a higher energy state at v_p. (c) Triplet (s-s) excitation: A string is broken up into two real rapidities v_{1h} and v_{2h}, each of which is describing a spinon. The two spinons combine into a triplet excitation as one of the spin rapidities Λ_α has been removed.

$$e^{iN_a P_b(v_\alpha)} \prod_{\beta(\neq\alpha)}^{N/2} e^{i\Phi(v_\alpha - v_\beta)} = 1 \ , \tag{3.3a}$$

where $P_b(v_\alpha)$ is the pseudomomentum of a bound pair ($\alpha = 1, \ldots, N/2$):

$$P_b(v) = \Phi(v) \tag{3.3b}$$

with $\Phi(v) = \pi - \theta(v)$ and $\theta(v) = 2\tan^{-1}(x)$.

The expression $\Phi(v_\alpha - v_\beta)$ in (3.3a) represents the scattering phase shift for a bound pair (with center of string) v_α off another bound pair v_β. The physical interpretation of Eq. (3.3a) is as follows: the phase shift (which consists of a free part and a scattering phase) acquired by carrying a bound state around the ring has to be equal to one.

It is more appropriate to rewrite (3.3a) as ($\alpha = 1, \ldots, N/2$)

$$N_a \theta(v_\alpha) = 2\pi I_\alpha + \sum_{\beta=1}^{N/2} \theta(v_\alpha - v_\beta) \ , \tag{3.3c}$$

where the quantum numbers I_α (integers or half-odd integers) arise by taking the logarithm of Eq. (3.3a). The bare quantum numbers I_α are integers if $N_a - M - 1$ is even and half odd integers (h.o.i.) otherwise. They are restricted to the interval

$$|I_\alpha| \leq I_{\max} \ , \tag{3.4}$$

where $I_{\max} = (N_a - M - 1)/2$. At half-filling, the number of available positions is $N_a/2$ (possible values of I_α in the interval $[-I_{\max}, I_{\max}]$), so that there is no freedom in distributing the numbers I_α.

We restrict our discussion to the case of a nondegenerate ground state. Away from half-filling, the number of available states ($2I_{\max}+1$) exceeds the number of actual pairs, so that freedom is left in the choice of the I_α's. The state of lowest energy is obtained by choosing $|I_\alpha|$ as close as possible to $I_{\max}$. The corresponding distribution of roots in the v plane is sketched in Fig. 2 (except for the roots at infinity). The pairs with $v \to \infty$ have an arbitrary weak "binding" energy and are present in the ground state for arbitrary filling n. We therefore expect the bond-breaking modes to be gapless (see Sec. IV).

In the limit of a large system ($N_a \to \infty, N/N_a$ finite), (3.3d) can be replaced by an integral equation of the Fredholm-type for the distribution of roots v_α on the real axis

$$\rho_0(v) = \frac{1}{\pi}\frac{1}{1+v^2} - \left[\int_{-\infty}^{-Q_0} + \int_{Q_0}^{\infty}\right] dv' \frac{1}{\pi}\frac{1}{1+(v-v')^2}\rho_0(v') \ , \tag{3.5a}$$

where Q_0 is determined from

$$\left[\int_{-\infty}^{-Q_0} + \int_{Q_0}^{\infty}\right] dv\, \rho_0(v) = \frac{n}{2} \ . \tag{3.5b}$$

For analytic purposes, it is more convenient to transform Eq. (3.5a) into the following form:

$$\rho_0(v) = 2R(2v) + \int_{-Q_0}^{Q_0} dv' 2R(2[v-v'])\rho_0(v') \ , \tag{3.5c}$$

where $R(x)$ denotes Shiba's function[44]

$$R(x) = \frac{1}{4\pi}\int_{-\infty}^{\infty} d\omega \frac{e^{i\omega x/2}}{1+e^{|\omega|}} \ . \tag{3.5d}$$

In (3.5c) we have extended the distribution $\rho_0(v)$ to the whole real axis, i.e., $\rho_0(v) = \rho_{\rm occ}(v) + \rho_h(v)$ where $\rho_{\rm occ}(v)$ is defined on the interval $(-\infty, Q_0] \cup [Q_0, \infty)$ whereas $\rho_h(v)$ denotes the distribution of unoccupied states on the interval $[-Q_0, Q_0]$. In Sec. V we show that the same function $\rho_h(v)$ describes the distribution of hole rapidities in Sutherland's formulation.[20]

The ground-state energy is given by

$$E_0 = -2tN_a \left[\int_{-\infty}^{-Q_0} + \int_{Q_0}^{\infty}\right] dv\, \rho_0(v) \left[2 - \frac{1}{1+v^2}\right] \tag{3.5e}$$

or on account of (3.5a) and (3.5b)

$$E_0 = 2tN_a\{\delta - \pi\rho_0(0)\} \tag{3.5f}$$

with $\delta = 1 - n$ the hole density. Equations (3.5a) or (3.5c) can be solved numerically by iteration for arbitrary filling n. The results are plotted in Fig. 3. The state parametrized by real rapidities as well as the ferromagnetic state have been included in Fig. 3. It is interesting to note, that above $n = \frac{2}{3}$ the reality of the rapidities enforces the state to acquire a finite magnetization (see Appendix A).

For a half-filled band ($Q_0 = 0$) the integral equation (3.5c) reduces to the simple expression

$$\rho_0(v) = 2R(2v) \ . \tag{3.6}$$

From (3.5f), the ground-state energy is $E_0 = -JN_a \ln 2$, in

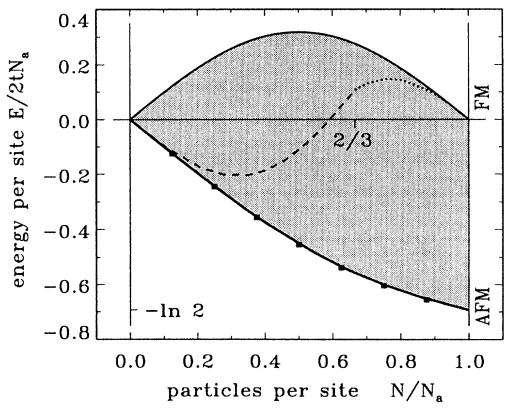

FIG. 3. Energy per site $E/2tN_a$ vs filling factor N/N_a. The ground state is a liquid of singlet pairs of varying range described by complex pairs of rapidities, see Fig. 2(a). The highest accessible state is the ferromagnetic state with real rapidities v_α and no spin rapidities Λ_α. The dashed line denotes the lowest singlet state with real rapidities v_α. This state is forced into a state with finite magnetization for a filling $N/N_a > \frac{2}{3}$ (dotted line). The filled squares denote the ground-state energy of a finite lattice of 16 sites obtained by exact diagonalization.

agreement with Hulthen's result for the antiferromagnetic Heisenberg chain.[43]

Near half-filling, the ground-state energy can be estimated from (3.5c). It increases linearly with the hole density ($\delta \ll 1$): $E_0(\delta)/N_a \approx E_0/N_a + A\delta$, where $A = 2t(1-\ln 2)$ is a positive constant. By standard arguments, it can be shown that $E_0(n)$ is an analytic and monotonically decreasing function of the band filling. Physically, it means that the energy gain due to the migration of the electrons through vacant sites is completely balanced by the loss in magnetic energy due to the insertion of holes. Notice that this is in contrast with the corresponding behavior in the large-U Hubbard model,[44] where the insertion of holes into a half-filled band allows the system to lower its energy.

In the low density limit we find that the energy behaves as $E_0(n)/N_a \approx -2tn$. In this regime, the supersymmetry of the model allows to construct an exact eigenstate (two-particle ground-state) by applying the up- and down-spin supercharges to the vacuum (see Sec. VI). The physics of the t-J model in the low density limit is that of noninteracting fermions. The transition between the strongly and weakly correlated regimes is achieved by simply varying the density n.

The dimensionless chemical potential $\mu(Q_0)$ (in units of $2t$) can be written as

$$\mu(Q_0) = -\left[1+\pi \frac{\partial \rho_0}{\partial Q_0}(0;Q_0) \Big/ \frac{\partial n}{\partial Q_0}(Q_0)\right], \quad (3.7a)$$

where

$$\frac{\partial \rho_0}{\partial Q_0}(v;Q_0) = [2R(2[v+Q_0])+2R(2[v-Q_0])]\rho_0(Q_0,Q_0) + \int_{-Q_0}^{Q_0} dv' 2R(2[v-v'])\frac{\partial \rho_0}{\partial Q_0}(v';Q_0) \quad (3.7b)$$

and

$$\frac{\partial n}{\partial Q_0}(Q_0) = -4\rho_0(Q_0;Q_0) + 2\left[\int_{-\infty}^{-Q_0} + \int_{Q_0}^{\infty}\right] dv \frac{\partial \rho_0}{\partial Q_0}(v;Q_0) . \quad (3.7c)$$

From (3.7), the chemical potential can be readily estimated at zero ($Q_0 = \infty$) and half-filling ($Q_0 = 0$), respectively, $\mu(\infty) = -1$ and $\mu(0) = \ln 2 - 1$. Both, the chemical potential and its derivative with respect to the density (the inverse of the compressibility) are shown in Fig. 4.

The compressibility κ is calculated from $\partial\mu/\partial n$ and using the relation[45]

$$\frac{1}{N_a}\frac{\partial^2 E_0}{\partial n^2} = \frac{\pi}{2}\frac{v_c}{K_\rho} , \quad (3.8)$$

where $v_c = v_{\text{holon}}$, we evaluate the charge critical exponent K_ρ which determines the algebraic decay of all correlation functions. The charge exponent K_ρ is shown in Fig. 5, where we have included for comparison the results obtained from exact diagonalization of a small cluster. The results for K_ρ obtained from (3.8) agree with the exact diagonalization calculations. Alternatively, by applying methods of conformal invariance, one can relate the compressibility to the "charge dressed matrix" element (in zero magnetic field) $\xi(Q_0)$[19,46,47]

$$\xi(Q_0)^2 = \pi v_c n^2 \kappa , \quad (3.9)$$

where $\xi(v)$ is solution of the integral equation[20]

$$\xi(v) = 1 + \int_{-Q_0}^{Q_0} dv' 2R(2[v-v'])\xi(v) . \quad (3.10)$$

The asymptotic behavior of K_ρ for a nearly half-filled band ($\delta \ll 1$) is readily estimated from either (3.8) or (3.9) and (3.10): $K_\rho \approx \frac{1}{2}(1+\delta)$.

To conclude this section we notice the following. From the point of view of the Bethe ansatz, the ground state is similar to that of the attractive Hubbard model as

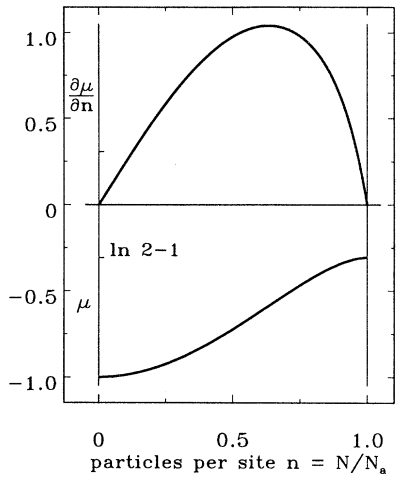

FIG. 4. Chemical point μ and its derivative $\partial\mu/\partial n$ ($\propto$ inverse compressibility) vs particle density $n = N/N_a$.

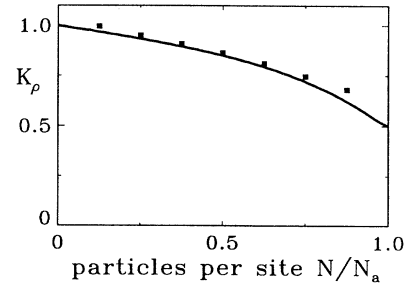

FIG. 5. Correlation exponent K_ρ as a function of particle density $n = N/N_a$. The value $K_\rho = 1$ in the dilute limit indicates free electronlike behavior. Whereas the strongly correlated Hubbard model is characterized by $K_\rho = \frac{1}{2}$ ($U \to \infty$) for all densities n the t-J model approaches this value only near half-filling.

both involve complex roots.[48] However, this is no longer true for the ground state in Sutherland's formulation (see Sec. V). Below, we demonstrate that the physics of the t-J model is more like that of the repulsive Hubbard model.[49]

IV. THE EXCITATION SPECTRUM

This section is devoted to a study of the low-lying part of the spectrum. For the sake of simplicity we consider a nondegenerate ground state, i.e., N_a even, N even, and $N/2$ odd. We find two types of elementary excitations.

(i) Charge excitations (occurring only away from half-filling): They are the analog of particle-hole excitations in a Fermi liquid with the difference that they carry no spin (transfer of bound singlet pairs). They are gapless.

(ii) Spin excitations (bond-breaking excitations with or without spin flip): they are gapless down to zero filling and pure spin only at half-filling. As the band filling decreases from $n=1$ to $n=0$, charge admixes so that they transform gradually into particle excitations.

In the present section we deal with Lai's form of the solution. In spite of the fact that this approach leads to involved manipulations of the spin excitations, it permits a simple physical picture. Sutherland's form of the solution allows a straightforward mathematical treatment of the excitation spectrum, but the physics is more difficult to extract from the latter.

A. The charge excitations

As emphasized in the previous section (see Appendix B), care is required when dealing with the singular roots of Eq. (2.11). In this section we start with Eq. (3.3d) and measure the crystal momentum with respect to the ground state. In Sec. III we showed that the ground state is uniquely defined by the choice $I_{\min}\le|I_\alpha|\le I_{\max}$, where $I_{\max}=(N_a-M-1)/2$ and $I_{\min}=(N_a-N-1)/2$. The number of available states is N_a-M and therefore the number of unoccupied states is the number of (physical) holes $N_h=N_a-N$ ($M=N/2$). An elementary excitation consists in transferring a particular $I_{\alpha_0}=I_h$ from the occupied region to a previously unoccupied state at the locus I_p: we denote by $\{I_\alpha\}$ the new distribution of bare quantum numbers. In the v plane, this process involves the transfer of a pair of complex conjugate roots from a state below the pseudo-Fermi surface to a state above the pseudo-Fermi surface [see Fig. 2(b)]. The pseudo-Fermi surface is defined as the set of points separating the occupied from the unoccupied regions in parameter space. To avoid confusion let us remind the reader that the effective Fermi surface is the locus of zero energy states in momentum space[50] and therefore the two sets of points need not coincide.

Retaining terms up to $O(N_a^{-1})$, Eq. (3.3d) can be written as

$$\rho(v)+\frac{1}{N_a}\delta(v-v_h)=\frac{1}{\pi}\frac{1}{1+v^2}-\frac{1}{N_a}\frac{1}{\pi}\frac{1}{1+(v-v_p)^2}-\left[\int_{-\infty}^{-Q}+\int_{Q}^{\infty}\right]dv'\rho(v')\frac{1}{\pi}\frac{1}{1+(v-v')^2}\ , \tag{4.1a}$$

where v_p and v_h denote, respectively, the positions of the transferred pair of the hole in the sea of two-strings associated with the bare quantum numbers I_p and I_h. The distribution $\rho(v)$ is normalized as follows ($M=N/2$, N even):

$$\left[\int_{-\infty}^{-Q}+\int_{Q}^{\infty}\right]dv\,\rho(v)=\frac{M-1}{N_a}\ . \tag{4.1b}$$

To rewrite (4.1a) in a more appropriate form we split $\rho(v)$ into a singular part and a smooth contribution[49]

$$\rho(v)=\rho_0(v)-\frac{1}{N_a}\rho_1(v)-\frac{1}{N_a}\delta(v-v_h)\ , \tag{4.2}$$

where $\rho_0(v)$ denotes the ground-state distribution at fixed Q and $\rho_1(v)$ a correction due to backflow.

On substitution of Eq. (4.2) into (4.1a) and using the Fourier-transform technique we find

$$\rho_1(v)=2R(2[v-v_p])-2R(2[v-v_h])+\int_{-Q_0}^{Q_0}dv'2R(2[v-v'])\rho_1(v')\ . \tag{4.3}$$

In (4.3) the function $\rho_1(v)$ has been extended to the whole real axis. The distribution of actual roots is however restricted to the region $(-\infty;-Q]\cup[Q;\infty)$ except for v_p which lies within the interval $[-Q,Q]$. By straightforward manipulations,[25] the energy of the excited state measured from the ground state is readily obtained:

$$\varepsilon(v_p,v_h)/2t=\pi\rho_1(0)+2[\mu(Q_0)+1]\left[\int_{-\infty}^{-Q_0}+\int_{Q_0}^{\infty}\right]dv\,\rho_1(v)\ , \tag{4.4}$$

where $\mu(Q_0)$ is the chemical potential. The momentum of the excited state measured from the ground state reads

$$P=-\frac{2\pi}{N_a}\sum_{\alpha=1}^{M}I_\alpha=\frac{2\pi}{N_a}(I_h-I_p)\ . \tag{4.5}$$

In Eq. (4.5) the ranges of I_h and I_p are such that $\pi-2k_F\le 2\pi/N_a|I_h|\le\pi-k_F$ and $2\pi/N_a|I_p|\le\pi-2k_F$ ($k_F=\pi n/2$). The relative crystal momentum of the excitation varies within the interval $0\le|P|\le 2\pi-3k_F$. To order N_a^{-1}, Eq. (4.5) can be written as

$$P(v_p,v_h)=2\pi\int_{v_p}^{v_h}dv\,\rho_0(v)\ , \tag{4.6}$$

where $|v_p|<Q<|v_h|$. Equations (4.4) and (4.6b) determine the dependence of the excitation energy on the momentum in a parametric form. Equation (4.3) has been solved numerically and the resulting dispersion rela-

tion is presented in Fig. 6 for various band fillings. The spectrum is gapless as expected. Above the density $n=\frac{2}{3}$ which marks a point of high symmetry, a gap of width $6k_F-2\pi$ opens in momentum, excluding excitations of this type with momenta between $2\pi-3k_F$ and $3k_F$. We wish to point out however that this apparent gap in crystal momentum is not real.[10] There exist low-energy charge excitations extending over the full Brillouin zone. A detailed analysis of the BAE shows that excitations involving the transfer of a bond pair in the presence of a broken bond (singlet) generate additional branches at $\pm 2k_F$ (modulo 2π) which become degenerate in the limit of a large system with the pure holon-antiholon spectrum described above. A discussion of this unusual situation is given in Sec. VI and for a thorough exposition of the mathematics the reader is referred to Ref. 25.

The effective Fermi surface for the charge excitations is at $|v|=Q$ (see Fig. 6) and coincides with the pseudo-Fermi surface. Keeping v_p fixed at the pseudo-Fermi surface (at Q) and moving v_h from one side of the pseudo-Fermi surface to the other one, we obtain the branch $\delta-\delta'$ (Fig. 6) with an effective Fermi surface spanning $4k_F$. In the same way, moving a bound pair v_p from Q to $-Q$ at fixed $v_h=Q$ involves a crystal momentum transfer:

$$P=2\pi\left[\int_{-\infty}^{-Q_0}+\int_{Q_0}^{\infty}\right]dv\,\rho_0(v)=2\pi-4k_F\ . \tag{4.7}$$

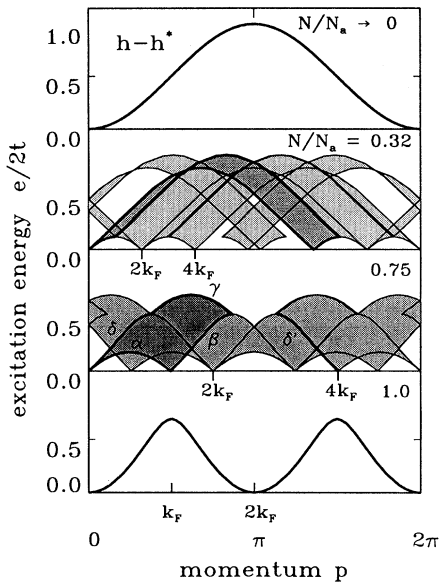

FIG. 6. Holon-antiholon (h-h^*) excitation spectrum for several values of the filling factor N/N_a. Starting with $v_h=v_p=Q$ [see Fig. 2(b)], branch α is obtained by moving v_p to $-Q$, branch β is due to moving v_h out to ∞, γ corresponds to moving v_p back to Q, and δ completes the loop as v_h is moved back to Q. The additional holon-antiholon branches at $\pm 2k_F$ (mod 2π) have been included in the figure. They correspond to the subfamily of lowest charge excitations involving broken bonds but are not elementary in a strict sense. However, they become degenerate with the pure holon-antiholon excitations in the thermodynamic limit.

This process corresponds to the branch α in Fig. 6.

The holon velocity can be calculated from

$$v_{\text{holon}}(P(v_h))=\frac{1}{2\pi\rho_0(v_h)}\frac{\partial\varepsilon}{\partial v_h}(v_h)\ , \tag{4.8a}$$

where

$$\frac{\partial\varepsilon}{\partial v_h}(v_h)=\pi\frac{\partial\rho_1}{\partial v_h}(0;v_h)+2[1+\mu(Q_0)]\left[\int_{-\infty}^{-Q_0}+\int_{Q_0}^{\infty}\right]dv\frac{\partial\rho_1}{\partial v_h}(v;v_h)\ . \tag{4.8b}$$

The function $\partial\rho_1/\partial v_h(0;v_h)$ obeys an integral equation which is readily inferred from (4.3). The holon velocity vs filling is shown in Fig. 7. From (4.5) and (4.8), it follows by expansion that the holon velocity at the pseudo-Fermi surface ($v_h=Q_0$) near half-filling is $v_{\text{holon}}\propto\delta$. We defer the detailed discussion of the spectrum for a nearly half-filled band to Sec. VI.

In the low density limit ($Q_0\to\infty$), only the anti-holon part of the spectrum survives and one obtains

$$\varepsilon(P)/2t=\tfrac{1}{2}(1-\cos(P))\ , \tag{4.9}$$

where $P=\pi-2\tan^{-1}(v_p)$ denotes the momentum of the excitation. Again, the antiholon velocity at the pseudo-Fermi surface $v_p=Q_0$ can be estimated as $n\to 0$. We find that $v_{\text{antiholon}}\propto n$.

B. The spin excitations

The construction of the spin excitation spectrum requires a careful study of the BAE. In this section we present a detailed analysis of the triplet channel. A similar procedure applies to the singlet channel.[25]

As discussed in Appendix B, the singular roots of Eq.

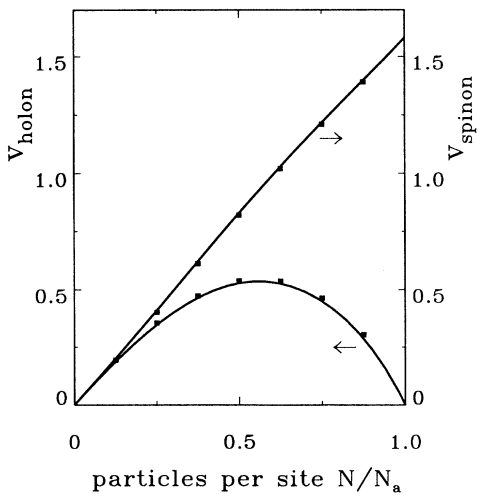

FIG. 7. Holon v_{holon} and spinon v_{spinon} velocity vs particle density $n=N/N_a$. The squares denote the results obtained from exact diagonalization for a system of 16 sites.

(2.11) must be considered separately in a rigorous treatment. For simplicity we assume again that the ansatz (3.1) covers all cases and measure the crystal momentum relatively to the ground state. Here, the manipulations are more involved than in the previous sections.

Let us consider the N-particle system in the ground state and break a particular bond by removing the corresponding Λ_α (which corresponds to the spin down of the pair) and simultaneously transferring the associated rapidities denoted by u_1 and u_2 onto the real axis [see Fig. 2(c)]. As a consequence, the real parts of the remaining two-strings shift with respect to the Λ's. The Bethe-ansatz equations (2.11) take the form ($M=N/2$, N even):

$$N_a\theta(v_\alpha)=2\pi I_\alpha+\sum_{\beta=1}^{M'}\theta(v_\alpha-\Lambda_\beta)\ , \tag{4.10a}$$

$$N_a\theta(2u_j)=2\pi I_j^u+\sum_{\beta=1}^{M'}\theta(2[u_j-\Lambda_\beta])\ , \tag{4.10b}$$

$$\sum_{j=1}^{2}\theta(2[\Lambda_\alpha-u_j])+\sum_{\beta=1}^{M'}\theta(\Lambda_\alpha-v_\beta)=2\pi J_\alpha+\sum_{\beta=1}^{M'}\theta(\Lambda_\alpha-\Lambda_\beta)\ , \tag{4.10c}$$

where $M'=M-1$ and the bare quantum numbers I_α are integers if N_a-M is even [half odd integers (h.o.i) otherwise] and the I_j^u are integers if N_a-M+1 is even (h.o.i., otherwise). The numbers J_α are always integers. The allowed ranges for I_α, I_j^u, and J_α are, respectively,

$$|I_\alpha|\le I_{\max}=\frac{N_a-M}{2}\ , \tag{4.11a}$$

$$|I_j^u|\le I_{\max}^u=\frac{N_a-M+1}{2}\ , \tag{4.11b}$$

$$|J_\alpha|\le 1\ , \tag{4.11c}$$

where $\alpha=1,\ldots,M'$. Careful analysis of Eqs. (4.10) shows that the choice of I_j^u, $j=1,2$ uniquely determines the set $\{J_\alpha\}$. The presence of holes in the distribution of numbers I_α drives a jump of unity in the numbers J_α exactly at the position of the holes.[25]

The momentum of the excited state consists of the contributions due to the M' unbroken bonds and those due to the broken bond:

$$P=\sum_{\alpha=1}^{M'}[\pi-\theta(v_\alpha)]+\sum_{j=1}^{2}[\pi-\theta(2u_j)]\ . \tag{4.12}$$

By exploiting Eqs. (4.10) the momentum can be written as

$$P=\pi-\frac{2\pi}{N_a}\sum_{\alpha=1}^{M'}(I_\alpha-J_\alpha)-\sum_{j=1}^{2}\theta(2u_j)+\frac{1}{N_a}\sum_{\alpha=1}^{M'}\sum_{j=1}^{2}\theta(2[u_j-\Lambda_\alpha])\ . \tag{4.13}$$

In (4.13) the momentum of the ground state has been subtracted.

We wish to calculate the spectrum induced by a particular choice of the numbers $\{I_j^u,I_\alpha\}$ at arbitrary filling.

Consider first the half-filled band. From (4.11), the numbers I_α are restricted to the interval $|I_\alpha|\le N_a/4$. The number of available states ($N_a/2+1$) exceeds by two the number of actual pairs ($N_a/2-1$). Therefore, the process of breaking one bond introduces two holes (unoccupied states) in the I_α, which we denote by I_α^h, $\alpha=1,2$. It turns out[25] that in this case the appropriate choice of the quantum numbers of the broken bond is

$$I_\alpha^h=I_j^u+\tfrac{1}{2} \tag{4.14}$$

for $j=1,2$.

At arbitrary values of the band filling, the number of available positions for the I_α in the excited state exceeds by two their number in the ground state. However, Eq. (4.14) no longer needs to be true, since we may choose the I_j^u outside the range of occupied states: $I_{\min}\le|I_\alpha|\le I_{\max}$, where $I_{\min}$ is determined from counting states ($I_{\min}=(N_a-N-1)/2$). This leads us to distinguish various cases, according to whether the unpaired rapidities u_1 and u_2 are embedded in the sea of two-strings or not.

In the thermodynamic limit, we replace (4.10) by two coupled integral equations for the distribution of the spin rapidities Λ and real part v of the electron rapidities

$$\rho(v)+\frac{1}{N_a}[\delta(v-v_{1h})+\delta(v-v_{2h})]=\frac{1}{\pi}\frac{1}{1+v^2}-\left[\int_{-\infty}^{-B}+\int_B^\infty\right]d\Lambda'\sigma(\Lambda')\frac{1}{\pi}\frac{1}{1+(v-\Lambda')^2}\ , \tag{4.15}$$

$$\left[\int_{-\infty}^{-B}+\int_B^\infty\right]d\Lambda'\sigma(\Lambda')\frac{1}{\pi}\frac{1}{1+(\Lambda-\Lambda')^2}+\frac{1}{N_a}[\delta(\Lambda-v_{1h})+\delta(\Lambda-v_{2h})]=\frac{1}{N_a}\left[\frac{1}{\pi}\frac{2}{1+4(\Lambda-v_{1h})^2}+\frac{1}{\pi}\frac{2}{1+4(\Lambda-v_{2h})^2}\right]+\left[\int_{-\infty}^{-Q}+\int_Q^\infty\right]dv'\rho(v')\frac{1}{\pi}\frac{1}{1+(\Lambda-v')^2}\ . \tag{4.16}$$

In (4.15) and (4.16) the rapidities v_{1h} and v_{2h} parametrize the holes in the sea of two-strings and, according to (4.15), are such that to $O(N_a^{-1})$ $v_{jh}=u_j$. On substitution of (4.16) into (4.15), (4.16) simplifies to a single integral equation for $\rho(v)$:

$$\rho(v)=2R(2v)-\frac{1}{N_a}\left[\frac{1}{2\cosh(\pi[v-v_{1h}])}+\frac{1}{2\cosh(\pi[v-v_{2h}])}\right]+\int_{-Q}^{Q}dv'\rho(v')2R(2[v-v']) . \tag{4.17}$$

It is convenient to split $\rho(v)$ into contributions of $O(1)$ and $O(N_a^{-1})$:

$$\rho(v)=\rho_0(v)-\frac{1}{N_a}\rho_1(v) . \tag{4.18}$$

As above, $\rho_0(v)$ is the ground-state distribution at fixed Q. From (4.17) and (4.18), we obtain a simple integral equation for $\rho_1(v)$:

$$\rho_1(v)=\frac{1}{2\cosh(\pi[v-v_{1h}])}+\frac{1}{2\cosh(\pi[v-v_{2h}])}+\int_{-Q_0}^{Q_0}dv'\rho_1(v')2R(2[v-v']) . \tag{4.19}$$

The energy of the excited state can be derived straightforwardly by manipulations similar to those of Ref. 49. We find

$$\varepsilon(v_{1h},v_{2h})/2t=\pi\rho_1(0)+2[1+\mu(Q_0)]\left[\left(\int_{-\infty}^{-Q_0}+\int_{Q_0}^{\infty}\right)dv\,\rho_1(v)-1\right] . \tag{4.20}$$

To calculate the crystal momentum relative to the ground state we assume without loss of generality $N/2$ odd. The appropriate choice of the $\{I_\alpha,J_\alpha\}$ yields to order $O(N_a^{-1})$ (Ref. 25)

$$\frac{2\pi}{N_a}\sum_{\alpha}(I_\alpha-J_\alpha)=-\frac{2\pi}{N_a}I_{\min} , \tag{4.21}$$

where $I_{\min}=(N_a-N-1)/2$. From (4.14) it follows that

$$P=2\pi-2k_F-\sum_{j=1}^{2}\theta(2v_{jh})+\left(\int_{-\infty}^{-Q_0}+\int_{Q_0}^{\infty}\right)dv\,\rho_0(v)\sum_{j=1}^{2}\theta(2[v_{jh}-v]) . \tag{4.22}$$

The spin excitation spectrum for various fillings is shown in Fig. 8.

The spinon velocity is calculated from

$$v_{\text{spinon}}(v_{1h})=-\frac{1}{2\pi\rho_s^0(v_{1h})}\frac{\partial\varepsilon}{\partial v_{1h}}(v_{1h}) , \tag{4.23}$$

where

$$\frac{\partial\varepsilon}{\partial v_{1h}}(v_{1h})=\pi\frac{\partial\rho_1}{\partial v_{1h}}(0)-[1+\mu(Q_0)]\int_{-Q_0}^{Q_0}dv\frac{\partial\rho_1}{\partial v_{1h}}(v) . \tag{4.24}$$

The integral equation for $\partial\rho_1/\partial v_{1h}(v)$ is readily obtained by taking the partial derivative of $\rho_1(v)$ with respect to v_{1h}. The spinon velocity versus filling is shown in Fig. 7.

In the limit of a half-filled band, an expansion in terms of the hole density ($\delta\ll 1$) is straightforward. We obtain

$$v_{\text{spinon}}(v_{1h})=\frac{\pi}{2}[1-\delta]\tanh(\pi v_{1h}) , \tag{4.25a}$$

$$P(v_{1h})=[1+\delta]\left[\frac{\pi}{2}-\tan^{-1}[\sinh(\pi v_{1h})]\right] . \tag{4.25b}$$

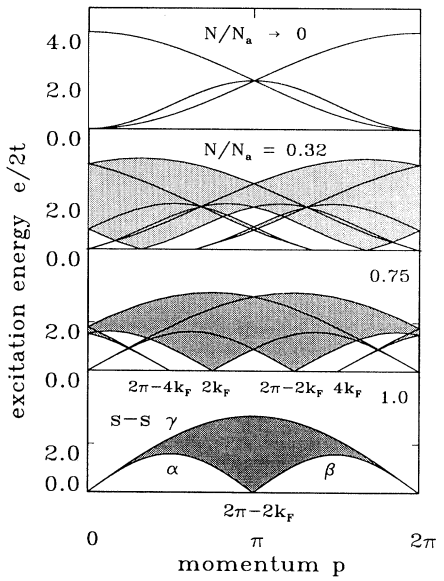

FIG. 8. Triplet (spinon-spinon, *s-s*) excitation spectrum for several values of the filling factor N/N_a. For $N/N_a\to 1$ the spectrum of the Heisenberg model is recovered. The branches α, β, and γ are obtained by starting with $v_{1h}=v_{2h}=\infty$ and moving $v_{1h}\to-\infty(\alpha)$, $v_{2h}\to\infty(\beta)$, and finally taking $v_{1h}=v_{2h}$ together back to ∞ (γ), see Fig. 1(c). The branch α is the spinon excitation spectrum spanning a Fermi surface of $2k_F$. The lowest (gapless) excitation is obtained by breaking a singlet pair at $\Lambda_\alpha=\pm\infty$, where the binding energy goes to zero. As $N/N_a\to 0$ the free particle triplet excitation spectrum is recovered.

Hence $v_{\text{spinon}}(p) \approx n(\pi/2)\cos(p)$. The spinon velocity near half-filling at the pseudo-Fermi surface ($v_{1h} \to \infty$ or $p=0$) is linear in the particle density, i.e., the insertion of holes into a half-filled band merely renormalizes the spinon velocity. The physical interpretation is as follows: the probability for a domain wall (spinon) to propagate to the nearest sites is proportional to $J_{\text{ren}} = Jn$ and the spinon velocity $\propto J_{\text{ren}}$. This behavior is in contrast with that of the large-U Hubbard model.[49]

In the low density limit, the spinon spectrum transforms into

$$\varepsilon(p_1,p_2)/2t = \varepsilon_0(p_1)+\varepsilon_0(p_2) , \tag{4.26}$$

where $\varepsilon_0(p) = 1-\cos p$. Notice that the particle-spectrum (4.26) is two parametric. At half-filling, Eq. (4.17) reduces to

$$\rho_1(v) = \frac{1}{2\cosh(\pi[v-v_{1h}])} + \frac{1}{2\cosh(\pi[v-v_{2h}])} . \tag{4.27}$$

From (3.6) and (4.20) the energy of the triplet excitation [the spin of the state is $S = S^z = (N_a - 2M')/2 = 1$] is given parametrically by

$$\varepsilon(v_{1h},v_{2h}) = \varepsilon(v_{1h})+\varepsilon(v_{2h}) , \tag{4.28a}$$

where $\varepsilon(v) = \pi/2\cosh(\pi v)$. The momentum is readily shown to be

$$P(v_{1h},v_{2h}) = p(v_{1h})+p(v_{2h}) , \tag{4.28b}$$

with $p(v) = \pi/2 - \tan^{-1}[\sinh(\pi v)]$. Setting $p_j = p(v_j)$, $j=1,2$, the dispersion relation can be written as

$$\varepsilon(p_1,p_2) = \frac{\pi}{2}(\sin p_1 + \sin p_2), \quad 0 \le p_1,p_2 \le \pi .$$

Hence, the triplet excitation reduces, at half-filling, to the two-parametric family of states of Ref. 51 (N even). We see that Lai's form of the solution is suited to physical interpretation. At arbitrary filling, the triplet (singlet) excitations corresponds to the process of breaking the singlet bonds with (without) spin flip. For various fillings, the excitation spectrum is shown in Fig. 4: it is gapless as expected. This is due to the presence of pairs with arbitrarily weak "binding" energy. We find that the effective Fermi surface for the spin excitations is at k_F, i.e., at $|v| = \infty$, and does not coincide with the pseudo-Fermi surface. Real rapidities embedded in the sea of singlet pairs, i.e., low energy excited states are identified, near half-filling, with spinons (chargeless spin-$\frac{1}{2}$ kinks). This terminology should be used with care, for the spinons are pure spin only at $n=1$. Isolated rapidities ($|u| < Q$) can be associated with real particle-excitations (carrying both spin and charge). Upon decreasing the band filling, the spinon spectrum gradually transforms into a real particle spectrum (Fig. 8). It is known that the spin excitations in the Hubbard model generate, in addition to the spin current, a charge current which can be evaluated in the large-U limit.[52] We expect that same phenomenon to occur in the t-J model. In Sec. VI we study the problem of separation of charge and spin degrees of freedom and demonstrate, by calculating the spinon-spinon phase shift, that the spin excitations behave as true spinons only at low energies and near half-filling.

V. SUTHERLAND'S REPRESENTATION

In Secs. III and IV we determined the ground state and the excitation spectra from the set of Eqs. (2.11). In this section we derive the same results from Eqs. (2.13) and establish the equivalence of the two representations. The advantage of Sutherland's formulation is twofold: (a) the ground state and part of the low-lying energy spectrum involves only real roots of (2.13) and so is technically more appealing;[53] (b) at half-filling (2.13) reduces to the known form of the solution of the Heisenberg spin-$\frac{1}{2}$ chain.[51] However, the physical picture of the excitations is more transparent in Lai's representation.

Taking the logarithm of Eq. (2.15) we obtain (N_a even)

$$N_a\theta(2v_\alpha) = 2\pi J_\alpha + \sum_{\beta=1}^{M_1}\theta(v_\alpha - v_\beta) - \sum_{j=1}^{M_2}\theta(2[v_\alpha - w_j]) , \tag{5.1a}$$

$$\sum_{\beta=1}^{M_1}\theta(2[w_j - v_\beta]) = 2\pi I_j , \tag{5.1b}$$

where $\theta(x) = 2\tan^{-1}(x)$. The J_α are integers provided $M_1 - M_2 + 1$ is even, h.o.i. otherwise, and I_j is integer if M_1 is even, h.o.i otherwise ($M_1 = N_h + N_\downarrow$, $M_2 = N_h$). In the limit of a large system, the energy of the t-J model in Sutherland's representation (in zero magnetic field) is given by [see (2.14) and (2.15)]

$$E = 2tN_a\left[1 - n - \int_{-\infty}^{\infty} dv\, \rho_s(v)\frac{\frac{1}{2}}{(\frac{1}{2})^2+v^2}\right] . \tag{5.1c}$$

We define the crystal momentum by $T\psi = e^{iP}\psi$, where ψ denotes the usual *fermion amplitude*. This prescription requires the addition of a constant to the expression (2.15) given by Sutherland[7]

$$P = \frac{2\pi}{N_a}\left[\sum_{\alpha=1}^{M_1} J_\alpha + \sum_{j=1}^{M_2} I_j\right] + \pi(N_a - M_1 - 1, \text{mod}(2)) , \tag{5.1d}$$

where $N_a - M_1 - 1 = N_\uparrow - 1$. To clarify this point, consider the case when one of the up spins is at $x = N_a$. A translation of the system by one lattice unit leads to the transfer of the up spin to the other side of the chain at $x=1$. In this process, a phase factor $(-1)^{N_\uparrow - 1}$ must be taken into account for the up spin has been carried through the $N_\uparrow - 1$ remaining up spins.

Again, it is crucial to count correctly the number of available states for the bare quantum numbers. They are restricted to the intervals $|J_\alpha| \le J_{\max}$ and $|I_j| \le I_{\max}$ with $J_{\max} = (N_a + M_2 - M_1 - 1)/2$ and $I_{\max} = M_1$. The maximal number of available positions for the $\{J_\alpha\}$ is $N_a - N_\downarrow$ and the number of unoccupied quantum numbers for an eigenstate (provided there are no complex roots, see below) with definite spin $S = S^z$ is $N_\uparrow - N_\downarrow = 2S^z$.

For simplicity we consider in this section excitations

above a nondegenerate ground state. A careful analysis shows that the ground state is degenerate in all cases but two: either for N_a even, M_1 odd and M_2 even, or for N_a odd, M_1 even and M_2 odd. The nondegenerate ground state (assume N_a even, N even, and $N/2$ odd) is uniquely specified by the choice $|J_\alpha| \leq J_{\max}$ and $|I_j| \leq I_{\max}$, with $J_{\max}=(N_a+N/2-1)/2$ and $I_{\max}=(N_h-1)/2$. In the limit of a large system, Eqs. (5.1) transform into coupled integral equations for the distribution of roots on the real axis:

$$\rho_s^0(v)=\frac{1}{\pi}\frac{\frac{1}{2}}{(\frac{1}{2})^2+v^2}+\int_{-Q_0}^{Q_0}dw'\rho_c^0(w')\frac{1}{\pi}\frac{\frac{1}{2}}{(\frac{1}{2})^2+(w'-v)^2}$$

$$-\int_{-\infty}^{\infty}dv'\rho_s^0(v')\frac{1}{\pi}\frac{1}{1+(v'-v)^2}\ , \tag{5.2a}$$

$$\rho_c^0(w)=\int_{-\infty}^{\infty}dv'\rho_s^0(v')\frac{1}{\pi}\frac{\frac{1}{2}}{(\frac{1}{2})^2+(v'-w)^2}\ . \tag{5.2b}$$

The normalization is such that

$$\int_{-\infty}^{\infty}dv\,\rho_s(v)=\frac{M_1}{N_a}\ , \tag{5.3a}$$

$$\int_{-Q_0}^{Q_0}dw\,\rho_c(w)=\frac{M_2}{N_a}\ . \tag{5.3b}$$

The limit of integration Q_0 alone determines the band filling. Applying the Fourier transform technique we can rewrite (5.2) as two uncoupled integral equations:

$$\rho_s^0(v)=\frac{1}{2\cosh(\pi v)}+\int_{-\infty}^{\infty}dv'\left[\frac{1}{\pi}\int_{-Q_0}^{Q_0}dw'\frac{\mathrm{sech}(\pi[w'-v])}{1+4(w'-v')^2}\right]\rho_s^0(v')\ , \tag{5.4a}$$

$$\rho_c^0(w)=2R(2w)+\int_{-Q_0}^{Q_0}dw'2R(2[w-w'])\rho_c^0(w')\ . \tag{5.4b}$$

An alternative and useful form of (5.2b) is

$$\rho_s^0(v)=\frac{1}{2\cosh(\pi v)}+\int_{-Q_0}^{Q_0}dw'\rho_c^0(w')\frac{1}{2\cosh(\pi[w'-v])}\ . \tag{5.5}$$

The integral equations (5.4b) and (3.5) are identical (provided we identify the limits of integration). Therefore, $\rho_c^0(w)$ and $\rho_0(v)$ (see Sec. III) denote the same analytic function over the whole real axis. They are complementary in the sense that the occupied roots on the w axis give precisely the unoccupied roots on the v axis, and vice versa. Notice however that the relationship between $\sigma(\Lambda)$ and $\rho_s^0(v)$ is more involved. Again, the ground-state energy can be written as

$$E_0=2t\{\delta-\pi\rho_c^0(0)\}\ , \tag{5.6}$$

where $\delta=1-n$ is the hole density. Equations (5.6) and (3.5f) are identical. The holon-antiholon spectrum is constructed in the same way as in Sec. IV A. A bare quantum number $I_\alpha=I_h$ is transferred from the occupied region to the locus I_p above the pseudo-Fermi surface. Again, writing the BAE in discrete form and taking the thermodynamic limit, we obtain[25]

$$\rho_s(v)=\frac{1}{2\cosh(\pi v)}+\frac{1}{N_a}\left[\frac{1}{2\cosh(\pi[v-w_p])}-\frac{1}{2\cosh(\pi[v-w_h])}\right]+\int_{-\infty}^{\infty}dv'\left[\frac{1}{\pi}\int_{-Q}^{Q}dw'\frac{\mathrm{sech}(\pi[v-w'])}{1+4(w'-v')^2}\right]\rho_s(v')\ , \tag{5.7a}$$

$$\rho_c(w)+\frac{1}{N_a}\delta(w-w_h)=2R(2w)+\frac{1}{N_a}2R(2[w-w_p])+\int_{-Q}^{Q}dw'2R(2[w-w'])\rho_c(w')\ . \tag{5.7b}$$

In order to compare the excitation spectrum with our previous results we express the energy in terms of the distribution $\rho_c(w)$ instead of $\rho_s(v)$ [see (5.1c)]. Splitting in (5.7) the terms of different orders and subtracting the ground-state energy, we arrive at the simple expression

$$\varepsilon(w_p,w_h)/2t=\pi\rho_c^1(0)-[\mu_h(Q_0)+1]\int_{-Q_0}^{Q_0}dw\,\rho_c^1(w)\ , \tag{5.8}$$

where $\mu_h(Q_0)$ is the chemical potential for the holes [see (4.15)]

$$\mu_h(Q_0)=-\mu(Q_0)\ . \tag{5.9}$$

The distribution $\rho_c^1(w)$ incorporates the effect of backflow in the charge distribution $\rho_c(w)=\rho_c^0(w)-(\delta(w-w_h)+\rho_c^1(w))/N_a$ and obeys to the integral equation

$$\rho_c^1(w)=2R(2[w-w_h])-2R(2[w-w_p])+\int_{-Q_0}^{Q_0}dw'2R(2[w-w'])\rho_c^1(w')\ . \tag{5.10}$$

On account of (5.9) and the relation [following from (5.10)]

$$\int_{-Q_0}^{Q_0} dw\,\rho_c^1(w) = -2\left[\int_{-\infty}^{-Q_0} + \int_{Q_0}^{\infty}\right] dw\,\rho_c^1(w)\ , \qquad (5.11)$$

it is seen that (5.8) and (4.4) are identical.

The momentum of the charge excitation can be expressed as in Sec. IV A

$$P = \frac{2\pi}{N_a}(I_p - I_h)\ , \qquad (5.12a)$$

where the ranges of the bare quantum numbers are such that

$$\frac{2\pi}{N_a}|I_h| \le \pi - 2k_F$$

and

$$\pi - 2k_F \le \frac{2\pi}{N_a}|I_p| \le \pi - k_F\ .$$

In the limit of a large system we obtain to $O(N_a^{-1})$

$$P(w_p, w_h) = 2\pi\int_{w_h}^{w_p} dw\,\rho_c^0(w)\ , \qquad (5.12b)$$

as in (4.6).

The spin excitations are straightforward in Sutherland's representation. We consider first the triplet excitation for which $N_\uparrow - N_\downarrow = 2$. Therefore, the spectrum is two-parametric. We denote by v_{1h}, v_{2h} the two holes (the missing rapidities) in the distribution $\rho_s(v)$. In the thermodynamic limit we find

$$\rho_s(v) + \frac{1}{N_a}[\delta(v - v_{1h}) + \delta(v - v_{2h})] = \frac{1}{\pi}\frac{\frac{1}{2}}{(\frac{1}{2})^2 + v^2} + \int_{-Q}^{Q} dw'\rho_c(w')\frac{1}{\pi}\frac{\frac{1}{2}}{(\frac{1}{2})^2 + (w' - v)^2} - \int_{-\infty}^{\infty} dv'\rho_s(v')\frac{1}{\pi}\frac{1}{1 + (v - v')^2}\ , \qquad (5.13a)$$

$$\rho_c(w) = \int_{-\infty}^{\infty} dv'\rho_s(v')\frac{1}{\pi}\frac{\frac{1}{2}}{(\frac{1}{2})^2 + (v' - w)^2}\ . \qquad (5.13b)$$

Separating contributions of different orders,

$$\rho_c(w) = \rho_c^0(w) - \frac{1}{N_a}\rho_c^1(w) \quad \text{and} \quad \rho_s(v) = \rho_s^0(v) - \frac{1}{N_a}[\delta(v - v_{1h}) + \delta(v - v_{2h})] + \frac{1}{N_a}\rho_s^1(v)\ ,$$

and applying the Fourier-transform technique we obtain

$$\rho_s^1(v) = 2R(2[v - v_{1h}]) + 2R(2[v - v_{2h}]) - \int_{-Q_0}^{Q_0} dw'\,\mathrm{sech}(\pi[w' - v])\frac{1}{\pi}\left[\frac{1}{1 + 4(w' - v_{1h})^2} + \frac{1}{1 + 4(w' - v_{2h})^2}\right] + \int_{-\infty}^{\infty} dv\,\rho_s^1(v')\left[\frac{1}{\pi}\int_{-Q_0}^{Q_0} dw'\frac{\mathrm{sech}(\pi[v - w'])}{1 + 4(w' - v')^2}\right]\ , \qquad (5.14a)$$

$$\rho_c^1(w) = \frac{1}{2\cosh(\pi[w - v_{1h}])} + \frac{1}{2\cosh(\pi[w - v_{2h}])} + \int_{-Q}^{Q} dw'\rho_c^1(w')2R(2[w - w'])\ . \qquad (5.14b)$$

For the excitation energy we find

$$\varepsilon(v_{1h}, v_{2h})/2t = \pi\rho_c^1(0) - [1 - \mu_h(Q_0)]\int_{-Q_0}^{Q_0} dw\,\rho_c^1(w)\ . \qquad (5.15)$$

From (5.14b) it follows that

$$\int_{-Q_0}^{Q_0} dw\,\rho_c^1(w) = -2\left[\left[\int_{-\infty}^{-Q_0} + \int_{Q_0}^{\infty}\right] dw\,\rho_c^1(w) - 1\right]\ . \qquad (5.16)$$

On account of (5.9) and (5.16) the identity of Eqs. (4.20) and (5.15) is easily verified. The momentum of the excitation is given by

$$P = 2\pi - 2k_F - \frac{2\pi}{N_a}(J_{h1} + J_{h2})\ , \qquad (5.17a)$$

with $2\pi/N_a|J_{1,2h}| \le \pi - k_F$, or in the limit of a large system

$$P(v_{1h}, v_{2h}) = 2\pi - 2k_F - 2\pi\left[\int_0^{v_{1h}} dv\,\rho_s^0(v) + \int_0^{v_{2h}} dv\,\rho_s^0(v)\right]\ . \qquad (5.17b)$$

The spin singlet excitation requires more algebra. As in the Heisenberg AFM chain, these elementary excitations involve a pair of complex conjugated roots in the v plane $v^{\pm} = v_s \pm i/2 + O(e^{-\varepsilon N_a})$. Equations (5.1a) and (5.1b) have to be replaced by

$$N_a\theta(2v_\alpha)=2\pi J_\alpha+\sum_{\beta=1}^{M_1-2}\theta(v_\alpha-v_\beta)-\sum_{j=1}^{M_2}\theta(2[v_\alpha-w_j])$$
$$+\theta(\tfrac{2}{3}[v_\alpha-v_s])+\theta(2[v_\alpha-v_s])\ , \tag{5.18a}$$

$$\sum_{\beta=1}^{M_1-2}\theta(2[w_j-v_\beta])+\theta(w_j-v_s)=2\pi I_j\ , \tag{5.18b}$$

where J_α are integers if M_1-M_2+1 even (h.o.i. otherwise) and I_j are integers if M_1-1 is even (h.o.i. otherwise). The sets $\{J_\alpha\}$ and $\{I_j\}$ are restricted to the intervals $|J_\alpha|\le(N_a-M_1+M_2-1)/2$ and $|I_j|\le(M_1-1)/2$. Again, the excitation is two-parametric. The center of the string v_s is determined from the equation

$$N_a\theta(v_s)=\sum_{\beta=1}^{M_1}[\theta(\tfrac{2}{3}[v_s-v_\beta])+\theta(2[v_s-v_\beta])]$$
$$-\sum_{j=1}^{M_2}\theta(v_s-w_j)\ . \tag{5.18c}$$

The energy and momentum of the excitation are given, respectively, by

$$E=2tN_a\left[1-n-\int_{-\infty}^{\infty}dv\,\rho_s(v)\frac{\frac{1}{2}}{(\frac{1}{2})^2+v^2}-\frac{1}{N_a}\frac{1}{1+v_s^2}\right]\ , \tag{5.19a}$$

$$P=\sum_{\alpha=1}^{M_1-2}2\theta(v_\alpha)+[\pi+2\theta(v_s)]\ . \tag{5.19b}$$

On account of Eqs. (5.18) the crystal momentum can be written as

$$P=2\pi-2k_F-\frac{2\pi}{N_a}(J_{h1}+J_{h2})\ . \tag{5.19c}$$

Equation (5.19c) coincides with (5.17a).

In the thermodynamic limit, Eqs. (5.18) transform into

$$\rho_s(v)+\frac{1}{N_a}[\delta(v-v_{1h})+\delta(v-v_{2h})]=\frac{1}{\pi}\frac{\frac{1}{2}}{(\frac{1}{2})^2+v^2}-\frac{1}{N_a}\left[\frac{1}{\pi}\frac{\frac{3}{2}}{(\frac{3}{2})^2+(v-v_s)^2}+\frac{1}{\pi}\frac{\frac{1}{2}}{(\frac{1}{2})^2+(v-v_s)^2}\right]$$
$$+\int_{-Q}^{Q}dw\,\rho_c(w)\frac{1}{\pi}\frac{\frac{1}{2}}{(\frac{1}{2})^2+(v-w)^2}-\int_{-\infty}^{\infty}dv'\rho_s(v')\frac{1}{\pi}\frac{1}{1+(v-v')^2}\ , \tag{5.20a}$$

$$\rho_c(w)=\frac{1}{N_a}\frac{1}{\pi}\frac{1}{1+(v_s-w)^2}+\int_{-\infty}^{\infty}dv'\rho_s(v')\frac{1}{\pi}\frac{\frac{1}{2}}{(\frac{1}{2})^2+(w-v')^2}\ , \tag{5.20b}$$

$$\theta(v_s)=\int_{-\infty}^{\infty}dv\,\rho_s(v)[\theta(\tfrac{2}{3}[v_s-v])+\theta(2[v_s-v])]-\int_{-Q}^{Q}dw\,\rho_c(w)\theta(v_s-w)\ . \tag{5.20c}$$

By Fourier transformation, it is readily shown that

$$\rho_s(v)=h(v)+\int_{-Q}^{Q}dw\,\rho_c(w)\frac{1}{2\cosh(\pi[v-w])}\ , \tag{5.21a}$$

where

$$h(v)=\frac{1}{2\cosh(\pi v)}-\frac{1}{N_a}\left[\delta(v-v_{1h})+\delta(v-v_{2h})+\frac{1}{\pi}\frac{\frac{1}{2}}{(\frac{1}{2})^2+(v-v_s)^2}+2R(2[v-v_{1h}])+2R(2[v-v_{2h}])\right]\ . \tag{5.21b}$$

On substitution of (5.21b) into (5.20b) we find

$$\rho_c(w)=2R(2w)-\frac{1}{N_a}\left[\frac{1}{2\cosh(\pi[w-v_{1h}])}+\frac{1}{2\cosh(\pi[w-v_{2h}])}\right]+\int_{-Q}^{Q}dw'\rho_c(w')2R(2[w'-w])\ . \tag{5.21c}$$

Again, separating contributions of different orders, we arrive at the following expressions for the back-flow distributions:

$$\rho_s^1(v)=2R(2[v-v_{1h}])+2R(2[v-v_{2h}])-\frac{1}{\pi}\frac{\frac{1}{2}}{(\frac{1}{2})^2+(v-v_s)^2}+\int_{-Q}^{Q}dw\,\rho_c^1(w)\frac{1}{2\cosh(\pi[v-w])}\ , \tag{5.21d}$$

$$\rho_c^1(w)=\frac{1}{2\cosh(\pi[w-v_{1h}])}+\frac{1}{2\cosh(\pi[w-v_{2h}])}+\int_{-Q}^{Q}dw'\rho_c^1(w)2R(2[w'-w])\ . \tag{5.21e}$$

The center of the string v_s is determined by substituting the expression (5.21a) for $\rho_s(v)$ into (5.20c): the terms of $O(1)$ cancel out whereas those of $O(1/N_a)$ imply that

$$\theta(2[v_s - v_{1h}]) + \theta(2[v_s - v_{2h}]) = 0 \ . \tag{5.22a}$$

In other words, the center of the string at arbitrary filling is given by

$$v_s = \frac{v_{1h} + v_{2h}}{2} \ , \tag{5.22b}$$

as in the case of the AFM Heisenberg chain.[51] Notice that Eq. (5.21e) for $\rho_c^1(w)$ agrees with the corresponding equation for the charge back-flow distribution in the triplet case [see (5.14b)]. On substitution of (5.21) into (5.19a), it is readily shown that the contribution of the string to the energy cancels out. We therefore obtain for the energy of the excitation the same expression as (5.8), and so the triplet and singlet excitations are degenerate for arbitrary band filling. This degeneracy is a consequence of the spin-SU(2) symmetry and supports the interpretation according to which the triplet and singlet excitations correspond to the symmetric, respectively, antisymmetric combinations of the two spinons. The symmetry can be lowered by applying a magnetic field. As a consequence, the degeneracy is lifted and a gap arises between the triplet and singlet spectra.[25,24]

In a recent work Kawakami and Yang[20] applied the technique of conformal invariance to determine the exponents of the large distance behavior of correlation functions in the t-J model. In their paper, the use of Lai's form of the solution is made. Alternatively, the method of Woynarovich[18] to evaluate the finite-size corrections to the energy can be applied advantageously to Sutherland's form of the solution which involves only real roots at low energies.

Motivated by the failure of Fermi liquid theory in one dimension, Haldane developed in the early eighties the concept of Luttinger liquid.[17] For a one-dimensional system without internal symmetry, the central result of the Luttinger liquid theory is that a single renormalized coupling parameter e^{ϕ} controls the exponents of correlation functions. The fundamental content of the theory can be expressed in an equation which relates the three spectral velocities v_S (sound wave velocity of collective density excitations), v_N, and v_J (associated with charge and spin current-carrying excitations, respectively)

$$v_S = (v_N v_J)^{1/2} \ ,$$

which can be used to define the coupling parameter e^{ϕ} as

$$v_N = v_S e^{-2\phi}, \quad v_J = v_S e^{2\phi} \ .$$

The appropriate generalization of the Luttinger liquid concept to systems with internal symmetry, i.e., t-J model, is provided by the finite-size scaling in conformal field theory. To illustrate this point let us define the velocity matrices

$$V_N = (Z^T)^{-1} V Z^{-1} \ , \tag{5.23a}$$

$$V_J = Z V Z^T \ , \tag{5.23b}$$

where V is a diagonal matrix with matrix elements v_c and v_s, the holon and spinon velocities at the pseudo-Fermi surface. Z denotes the dressed charge matrix as defined in Refs. 18 and 19. In fact, it is readily shown that the dressed charge matrix is nothing but the scattering matrix for the elementary excitations of the model at the corresponding pseudo-Fermi surfaces.[25] As in the scalar case, the velocity-matrix V_J controls the mean current (charge and spin) and V_N is related to the susceptibilities.[19] The fundamental relation of the Luttinger theory now generalizes to

$$V_J V_N = Z V^2 Z^{-1} \tag{5.24}$$

and the renormalized coupling parameter of the theory is simply the dressed charge matrix, which determines the exponents of the asymptotic behavior of the correlation functions, as we know from conformal field theory.[19] Using Sutherland's representation, the finite-size scaling of the energy and momentum can be calculated as in Refs. 18 and 19 and in terms of the three-spectral velocity matrices can be written, in analogy with Haldane's formulation,[17] as

$$E(\Delta N, D) - E_0 = \frac{2\pi}{N_a} \left[\frac{1}{4} \Delta N^T V_N \Delta N + D^T V_J D + u^T V \sum_{\alpha = \pm} N^{\alpha} \right] , \tag{5.25a}$$

$$P(\Delta N, D) - P_0 = \frac{2\pi}{N_a} \left[\Delta N D + F^T D + u^T \sum_{\alpha = \pm} \alpha N^{\alpha} \right] , \tag{5.25b}$$

where the superscript T denotes transposition and u, ΔN, D, F, $N^{\pm}$ are two-component vectors defined as $u_1 = u_2 = 1$, $\Delta N_{1,2} = \Delta N_{c,s}$, $D_{1,2} = D_{c,s}$, $F_{1,2} = 2q_{c,s}^F$, and $N_{1,2}^{+} = N_{c,s}^{+}$. The pseudo-Fermi surfaces $q_{c,s}^F$ for the charge and spin excitations are given for the t-J model by $q_c^F = \pi - k_{F\downarrow} - k_{F\uparrow}$ and $q_s^F = \pi - k_{F\downarrow}$. The remaining notation is that of Ref. 19.

For the t-J model in zero magnetic field, the spectral velocities take the form

$$V_J = \begin{bmatrix} 2K_\rho v_c & K_\rho v_c \\ K_\rho v_c & \dfrac{K_\rho v_c}{2} + \dfrac{v_s}{2} \end{bmatrix} , \tag{5.26a}$$

$$V_N = \begin{bmatrix} \dfrac{v_c}{2K_\rho} + \dfrac{v_s}{2} & -v_s \\ -v_s & 2v_s \end{bmatrix} , \tag{5.26b}$$

where K_ρ is the charge exponent introduced at the end of Sec. III. The diagonal matrix elements of V_J, i.e., $v'_{\text{holon}} = 2K_\rho v_c$ and $v'_{\text{spinon}} = v_s/2 + K_\rho v_c/2$ represent velocities associated with the $2q_c^F = 2\pi - 4k_F$ and $2q_s^F = 2\pi - 2k_F$ processes, respectively, and are defined as the corresponding excitation energy normalized by the unit momentum $2\pi/N_a$. This velocities versus band filling are

shown in Fig. 9. The mean charge and spin currents are then given by

$$j_c \propto v'_{\text{holon}}[2D_c + D_s] , \tag{5.27a}$$

$$j_s \propto v'_{\text{spinon}} 2D_s + v'_{\text{holon}} D_c . \tag{5.27b}$$

Therefore, a spin current-carrying state with $D_s \neq 0$ and $D_c = 0$ involves a charge current $\propto v'_{\text{holon}} D_s$. This fact corroborates our picture of the spin excitations according to which the low energy part of the spectrum has a predominantly spin character near half-filling where $v'_{\text{holon}} \ll v'_{\text{spinon}}$.

VI. THE EXCITATION SPECTRUM NEAR HALF-FILLING

The analysis of the excitation spectrum near half-filling deserves particular attention. Anderson has emphasized the concept of separation of charge and spin degrees of freedom in strongly correlated systems. Anderson's idea finds its justification on a subtle analysis of the excitation spectrum of the one-dimensional large-U Hubbard model.[50,54] The key step in his approach is to recognize that the low energy part of the spectrum can be thought of as consisting of parametrically independent solitonlike excitations carrying separately charge (holons) and spin (spinons).

For the t-J model, the main results can be summarized as follows: the concept of separation of charge and spin degrees of freedom is applicable only at low energies and near half-filling. To illustrate this phenomenon the case of one hole in an even chain is considered.

Furthermore, the holon and spinon spectra in odd chains show interesting structure. A pure spinon spectrum in an odd chain extends in momentum space over a region of width $2k_F = \pi$. However, exact numerical diagonalization of small clusters[42] shows the existence of spinonlike excitations covering the full Brillouin zone. The additional branch can be explained in terms of composite excitations involving singlet broken bonds. The insertion of a hole into the odd chain leads to a pure holon spectrum (over a nondegenerate ground state) spanning $2k_F = \pi$. Again, numerical calculations indicate a holonlike spectrum extending over the whole Brillouin zone. The full spectrum is generated by taking into account composite excitations involving the rearrangement of the spin degrees of freedom.

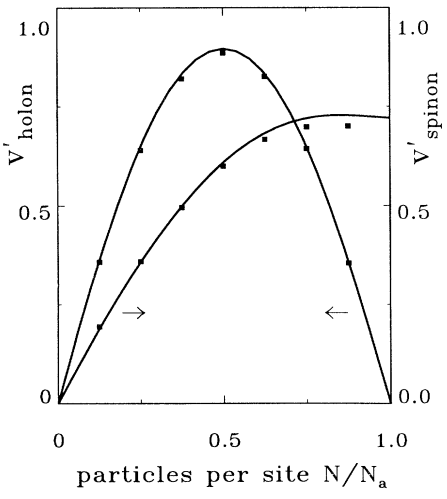

FIG. 9. Holon v'_{holon} and spinon v'_{spinon} velocity vs particle density $n = N/N_a$. The quantities v'_{holon} (v'_{spinon}) are defined as the finite-size excitation energies at $4k_F$ ($2k_F$) of the charge (spin) excitation, normalized by the momentum unit $2\pi/N_a$. The squares denote the results obtained from exact diagonalization for a system of 16 sites.

The spin excitations described in Secs. IV B and V alter gradually their spinon character as the band filling is decreased. Owing to this peculiar behavior, counting the number of degrees of freedom in the problem is not a simple task and may easily lead to erroneous conclusions. For instance, it is confusing at first sight that the number of states in the spin spectrum (see Fig. 8) increases as the filling decreases, in contrast to the Hubbard model. The reason for this unusual situation is given below.

In order to elucidate the mechanism of separation of charge and spin degrees of freedom in the t-J model, we investigate excitations involving a change in particle number (doping). The simplest case is certainly obtained by doping an even chain with a single hole. We start with a half-filled band, assume a nondegenerate ground state (M_1 odd and M_2 even), and insert into the system a single hole.[55] For clarity we deal with Sutherland's representation. In the presence of one hole, the Bethe-ansatz equations (5.1) read

$$N_a \theta(2v_\alpha) = 2\pi J_\alpha - \theta(2[v_\alpha - w]) + \sum_{\beta=1}^{M_1} \theta(v_\alpha - v_\beta) , \tag{6.1a}$$

$$\sum_{\beta=1}^{M_1} \theta(2[w - v_\beta]) = 2\pi I , \tag{6.1b}$$

where the quantum numbers I and J_α are always half odd integers. They are restricted to the intervals $|I| \leq N_a/4$, $|J_\alpha| \leq N_a/4$. The number of available states for the J_α is $(N_a/2+1)$ whereas the number of actual roots is $N_a/2$. Therefore, there is one empty state $J_h(v_h)$ which parametrizes the spin degree of freedom. On the other hand, I is associated with the charge degree of freedom (holon). More explicitly, a general state is determined from

$$\{J_\alpha\} = \left[-\frac{N_a}{4}, \ldots, [^{J_h}], \ldots, -\frac{1}{2}, \frac{1}{2}, \ldots, \left[\frac{N_a}{4} - 1 \right] \right] \tag{6.2a}$$

and

$$I \varepsilon \left[-\frac{N_a}{4}, \frac{N_a}{4} \right] , \tag{6.2b}$$

where J_h denotes the unoccupied quantum number. The crystal momentum of this state is given by

$$P=\frac{2\pi}{N_a}(I-J_h)\ . \tag{6.3}$$

The ground state is obtained for either choice

$$\{J_\alpha\}=\left[-\frac{N_a}{4},-\left[\frac{N_a}{4}-1\right],\ldots,-\frac{1}{2},\frac{1}{2},\ldots,\left[\frac{N_a}{4}-1\right]\right],\quad I=\frac{1}{2}\ ,$$

or

$$\{J_\alpha\}=\left[-\left[\frac{N_a}{4}-1\right],\ldots,-\frac{1}{2},\frac{1}{2},\ldots,\left[\frac{N_a}{4}-1\right],\frac{N_a}{4}\right],\quad I=-\frac{1}{2}\ ,$$

and so, the ground state of the N_a-1 particle system is twofold degenerate with momentum $P=\pm 2\pi/N_a([(N_a+2)/4])\approx\pm k_F$.

In the limit of a large system, the configuration of quantum numbers (6.2) yields

$$\rho_s(v)+\frac{1}{N_a}\delta(v-v_h)=\frac{1}{\pi}\frac{\frac{1}{2}}{(\frac{1}{2})^2+v^2}+\frac{1}{N_a}\frac{1}{\pi}\frac{\frac{1}{2}}{(\frac{1}{2})^2+(v-w)^2}-\int_{-\infty}^{\infty}dv'\rho_s(v')\frac{1}{\pi}\frac{1}{1+(v-v')^2}\ . \tag{6.4}$$

Substitution of $\rho_s(v)=\rho_s^0(v)+1/N_a[\rho_s^1(v)-\delta(v-v_h)]$ into (6.4) leads to

$$\rho_s^0(v)=\frac{1}{2\cosh(\pi v)}\ , \tag{6.5a}$$

$$\rho_s^1(v)=\frac{1}{2\cosh(\pi[v-w])}+2R(2[v-v_h])\ . \tag{6.5b}$$

The energy can be expressed directly in terms of $\rho_s(v)$ as (see Sec. V)

$$E=-t(N_a-2)-2tN_a\int_{-\infty}^{\infty}dv\,\rho_s(v)\left[\frac{\frac{1}{2}}{(\frac{1}{2})^2+v^2}-1\right]\ . \tag{6.6}$$

On substitution of (6.5) into (6.6) we find

$$E(v_h,w)=-2tN_a\ln 2+2t(1-2R(2w))+2t\frac{\pi}{2\cosh(\pi v_h)}\ . \tag{6.7}$$

Thus the ground-state energy is given by (see Sec. III)

$$E(v_h=\pm\infty,w=0)=-2tN_a\ln 2+2t(1-\ln 2)\ .$$

From (6.3) the momentum in the limit of a large system can be written as

$$p(v_h,w)=2\pi\int_0^w dw'\rho_c^0(w')-2\pi\int_0^{v_h}dv'\rho_s^0(v')\ , \tag{6.8}$$

where $\rho_c^0(w)$ denotes the distribution of *unoccupied* roots w whereas $\rho_s^0(v)$ denotes the distribution of *occupied* roots v in the ground state of the N_a-particle system [see (5.4b) and (5.5)]. From (6.7) and (6.8) the energy and momentum of the excited state is given additively by the energies and momenta of the individual kinks

$$\varepsilon(v_h,w)=2t[\varepsilon_{\text{holon}}(w)+\varepsilon_{\text{spinon}}(v_h)]\ , \tag{6.9a}$$

where $\varepsilon_{\text{holon}}(x)=\ln 2-2\pi R(2x)$ and $\varepsilon_{\text{spinon}}(x)=\pi/2\cosh(\pi x)$ denote the contributions of the holon and spinon, respectively, and

$$P(v_h,w)=p_{\text{holon}}(w)+p_{\text{spinon}}(v_h)\ , \tag{6.9b}$$

with the notation $p_{\text{holon}}(x)=2\pi F(2x)$ and $p_{\text{spinon}}(x)=-\tan^{-1}(\sinh(\pi x))$, where $F(x)=\int_0^x dy\,R(y)$.

From this simple algebra we infer that the one-hole excitation in a half-filled band is *two-parametric.* Upon doping, the system is left in an excited state of the N_a-1 particle system. The insertion of a hole with momentum $P=0$ produces a spinon (spin soliton of charge $q=0$ and spin $s=\frac{1}{2}$) at $\pm k_F$, and by crystal-momentum conservation a holon (charge soliton with charge $q=e$ and spin $s=0$) at $\mp k_F$ which is energetically unfavorable. The ground state of the N_a-1 particle system is degenerate and corresponds to a state with momentum $P=\pm\pi/2$, for which the charge and spin degrees of freedom of the hole have been separated. A physical picture of this mechanism of separation is as follows.[54] Consider an even chain of spins with short-range AFM order and remove, say, an up spin at site i. The vacancy left at position i is surrounded by a ferromagnetic (FM) alignment of the down spins. Now, let us propagate the hole to the nearest neighbor sites by applying the Hamiltonian to the system. After the hole has hopped by one lattice site, the hole is surrounded by an AFM alignment of the spins (holon) and a FM domain wall (spinon) arises on the adjacent sites. The holon carries an excess charge $q=e$ whereas the spinon carries an excess spin $s=\frac{1}{2}$. By further applying the Hamiltonian to the chain, it is easily seen that the spinon and holon propagate independently.

The low-energy hole spectrum is shown in Fig. 10 for a finite doping. At high energies the interaction of the spinons and holons is responsible for the recombination of charge and spin degrees of freedom and so the simple addition of the holon and spinon spectra is meaningless (dotted part of the spectrum in Fig. 10).

As in the Hubbard model,[56] the BAE dictate selection rules for the number of holons and spinons present in the system: $(-1)^{N_{\text{holon}}}(-1)^{N_{\text{spinon}}}=(-1)^{N_a}$, where N_{holon}, N_{spinon} denote the number of holons and spinons, respectively. The topological character of the spin solitons imposes constraints on their number although the latter is not fixed (in zero-magnetic field, the chemical potential is zero): for even N, the spinons occur in pairs whereas for odd N their number is always odd (see Sec. IV). The chemical potential for the holons is $\mu_{\text{holon}}=-\mu_{\text{electron}}$ and so their number in the holon Fermi sea is fixed: $N_{\text{holon}}=N_{\text{holes}}$.

In order to understand the peculiar features of the spi-

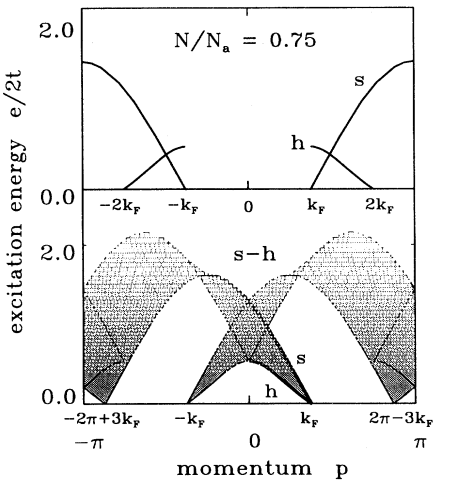

FIG. 10. Single particle (*s-h*) excitation spectrum. Removing a particle leaves the system back in an excited state characterized by a spinon *s* and a holon *h*. Top: holon and spinon excitation spectra with Fermi surfaces at $2k_F$ and at k_F, respectively. Bottom: combination of the *s* and *h* excitation spectra into a real particle (*s-h*) excitation spectrum. The state at k_F ($3k_F$) is a combination of a $2k_F$ holon and a $-k_F$ (k_F) spinon. The spectrum has been folded back into the first Brillouin zone.

non and holon spectra we now consider the case of a chain with an odd number of sites N_a.

Assume first a half-filled band with $M_1=(N_a-1)/2$ odd. The quantum numbers $\{J_\alpha\}$ are h.o.i. and such that $|J_\alpha|\leq(N_a-1)/4$. By counting the number of available positions for the $\{J_\alpha\}$, it is readily seen that the state is one-parametric. The ground state is degenerate and is obtained for either choice

$$\{J_\alpha\}=\left[-\frac{N_a-1}{4},\ldots,-\tfrac{1}{2},\tfrac{1}{2},\ldots,\frac{N_a-5}{4}\right]$$

or

$$\{J_\alpha\}=\left[-\frac{N_a-5}{4},\ldots,-\tfrac{1}{2},\tfrac{1}{2},\ldots,\frac{N_a-1}{4}\right].$$

The crystal momentum of the ground state is clearly $P=\pm\pi/2$ (modulo 2π). The unoccupied quantum number J_h parametrizes the spinon. The dispersion relation of the excitation is simply given by $\varepsilon(v_h)=2t\varepsilon_{\text{spinon}}(v_h)$, $P(v_h)=\pi+p_{\text{spinon}}(v_h)$ [see (6.9)]. Thus, the spinon spectrum extends over a region of momentum space of width $2k_F=\pi$.

As mentioned above, there is a simple and physical picture of the spinon as a FM domain wall in an AFM background of spins.[57] The domain wall propagates on either the even- or odd-numbered sublattices. Periodic boundary conditions ensure that after one turn around the ring, say on the even-numbered sublattice, the propagation takes place on the odd-numbered sublattice and vice versa.

This picture however indicates that the number of states in the one-spinon spectrum does not reproduce the right number of degrees of freedom. To elucidate this point a detailed analysis of the BAE is required.[25] From the previous section we know that spin excitations parametrized by a pair of complex roots $v^{\pm}=v_s\pm i/2+O(e^{\varepsilon N_a})$ are singlet and become degenerate with the triplet excitations in the limit of a large system for even chains. Consider now such singlet excitations in an odd chain. The BAE are given in (5.18) with the numbers $\{J_\alpha\}$ as h.o.i. (M_1 odd). They are restricted to the interval $|J_\alpha|\leq(N_a-1)/4$ and so the excitation is three-parametric. The manifold of excited states with the lowest energy is obtained by choosing two unoccupied quantum numbers at $\pm(N_a-1)/4$ and letting one unoccupied number vary over the allowed range of parameter space. The energy dispersion for this class of states is $\varepsilon(v_h)=2t\varepsilon_{\text{spinon}}(v_h)$, $p(v_h)=p_{\text{spinon}}(v_h)$. Therefore, the one-parametric subfamily of states is degenerate with the pure spinon spectrum and the presence of the complex roots only affects the crystal momentum by a constant $2k_F$.[58] The full spinon spectrum is shown in Fig. 11(a).

The physical picture which arises from these considerations is as follows: a FM domain wall in a pure AFM background of spins moves undisturbed within the same sublattice (open boundary conditions) whereas a spinon does not. The propagation of the spinon takes place on both sublattices, however for a finite chain the spinon propagates preferentially on the same sublattice. The propagation of the spinon on the adjacent sublattice is accompanied by the emission of pairs of antiparallel FM domain walls, i.e., pairs of spinons in a singlet state.

Let us now insert one physical hole into the odd chain ($N=N_a-1$). In this case we have $M_1=(N_a+1)/2$ even and $M_2=1$ odd, and the J_α are h.o.i. and I is integer. The number of available positions in the J_α is exactly equal to the number of rapidities v_α. Therefore, the state is one-parametric and the dispersion relation for the holon is given by $\varepsilon(w)=2t\varepsilon_{\text{holon}}(w)$ $P(w)=p_{\text{holon}}(w)$.

In real space, the holon has been pictured as a hole surrounded by an AFM configuration of the neighboring

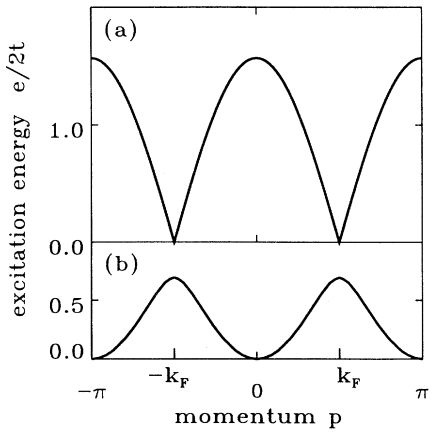

FIG. 11. (a) Single spinon spectrum in an odd chain at half filling and (b) single holon excitation spectrum in an odd chain near half filling.

spins, allowing for a π-phase shift of the spin arrangement. *A priori,* the holon can propagate on every site of the lattice without disturbing the AFM arrangement of the spins and so we expect N_a states in the holon spectrum. Counting the number of degrees of freedom is a confusing task, for the holon spectrum covers only half of the Brillouin zone. This apparent discrepancy is solved by invoking states with complex roots. Consider the holon spectrum in the presence of one pair of complex roots $v^{\pm}=v_s \pm i/2$. The corresponding BAE are then given by Eqs. (5.18) where $M_1=(N_a+1)/2$ (even) and $M_2=1$ (odd). The bare quantum numbers describing the distribution of real roots are such that $|J_\alpha| \leq (N_a-1)/4$ and $|I| \leq (M_1-1)/2$, and the family of states generated in this manner is three-parametric. Again, the manifold of lowest energy states is one-parametric and the dispersion relation is simply $\varepsilon(w)=2t\varepsilon_{\rm holon}(w), P(w)=\pi+p_{\rm holon}(w)$. Notice that this spectrum is degenerate (in the thermodynamic limit only) with the pure holon spectrum discussed previously but that the crystal momentum differs by a constant of that of the pure holon spectrum. In the limit of a large system the holon spectrum of the t-J model is $2k_F$ periodic [see Fig. 11(b)] in momentum space in contrast with that of the Hubbard model which is $4k_F$ periodic.[49,56] The physical content can be expressed by saying that the propagation of the holon strongly couples to the spin degrees of freedom. Consider a single holon on the chain: on both sides of the holon we have a Heisenberg chain (periodic boundary conditions) with one open boundary. The propagation of the holon to the nearest sites involves the transfer of a spin from one end of the chain to the other: this process implies a rearrangement of the spin configuration over the whole chain. This picture indicates that the short-range AFM correlations in the t-J model strongly affect the holon dynamics. The effective masses near half-filling at the bottom[59] and top of the holon band follow from (6.9) (in units of $2t$): $m_{\rm ef}^{\rm bot}=4[\ln 2]^2/3\zeta(3)$, and $m_{\rm ef}^{\rm top}=-\frac{1}{4}$ where $\zeta(z)$ denotes the Riemann ζ function, and so: $|m_{\rm ef}^{\rm top}| \leq m_{\rm ef}^{\rm bot}$.

This analysis of the holon spectrum can be easily extended to arbitrary filling.[25] As mentioned in Sec. IV, the presence of a pair of spinons in a singlet state affects the momentum of the charge excitation and additional holon-antiholon branches arise at $\pm 2k_F$ (modulo 2π). These excitations are not elementary in a strict sense, since they involve the composition of two types of elementary processes. However, it is worth mentioning them: they reflect the fact that the coupling of charge and spin degrees of freedom in the t-J model is strong over a wide range of energies and momenta. This property is also manifest in the spin spectrum as is discussed below.

In Sec. IV we claimed that the spin excitations behave as spinons only at low energies. We wish now to show that at low enough energies the scattering phase shift between the spin-solitonlike excitations is identical to that which occurs between spinons (FM domain walls) in the AFM Heisenberg chain. As the band filling decreases from $n=1$ the energy region of the excitation spectrum with dominantly spinon character shrinks and finally collapses at zero filling. The spinon-spinon, the holon-holon, and the spinon-holon scattering phase shifts have been evaluated by Korepin's method.[47] For convenience we present the results in Sutherland's representation.[25,24] In particular, the spinon-spinon phase shift (as defined in Ref. 47) in the triplet state is given, up to an unimportant constant, by

$$\Phi_{st}(v_{1h},v_{2h})=2\pi F(2[v_{1h}-v_{2h}])-\int_{-Q_0}^{Q_0} dw' \frac{\tan^{-1}(2[w'-v_{2h}])}{\cosh(\pi[v_{1h}-w'])} + \int_{-\infty}^{\infty} dv'' \left[\frac{1}{\pi}\int_{-Q_0}^{Q_0} dw' \frac{\operatorname{sech}(\pi[v_{1h}-w'])}{1+4(w'-v'')^2}\right] \Phi_{st}(v'',v_{2h}) \ . \tag{6.10}$$

Notice that $\Phi_{st}(-v_{1h},-v_{2h})=-\Phi_s(v_{1h},v_{2h})$, as required by time reversal symmetry and that the expression (6.10) is Galilean invariant only at half-filling. Provided that

$$Q_0 \ll v_{1h}, v_{2h} \ , \tag{6.11}$$

the phase shift reads

$$\Phi_{st}(v_{1h},v_{2h}) \approx 2\pi F(2[v_{1h}-v_{2h}])+O(e^{-\pi|v_{1h}|}) \ . \tag{6.12}$$

In other words, Eq. (6.12) gives the phase shift for the spin excitations in the triplet channel of the Heisenberg AFM chain.[51] The same analysis applies to the singlet case.[25] Provided that condition (6.11) is fulfilled, the concept of spinons make sense. However, this condition may be violated as $n \to 0$, since then $Q_0 \to \infty$ and the last term on the RHS of (6.10) is no longer an exponentially small term. In the dilute limit the picture of the domain wall is poorly defined and the propagation of the spin excitation requires a substantial rearrangement of the charge degrees of freedom. In the Lieb and Wu solution of the Hubbard model,[3] the situation is different: the rapidities parametrizing the charge degrees of freedom $[v(k)=\sin(k)]$ are bounded. As a consequence, the spin spectrum in the Hubbard model has spinon character down to zero filling over a wide range of energies.[56]

A similar analysis applies to the scattering of holons off other holons and spinons. Near half-filling, the phase shift acquired by scattering a holon w off another holon w' can be approximated by[25]

$$\Phi_{cc}(w,w') \approx -2\pi F(2[w-w']) = p_{\rm holon}(w'-w) \ , \tag{6.13}$$

that is, the holon-holon scattering phase shift is identical (up to a sign) to the triplet spinon-spinon phase shift near half-filling: the holons behave as spinless spinons in this regime. For the scattering of a spinon off a holon we find

$$\Phi_{sc}(v_h,w)\approx-\tan^{-1}(\sinh(\pi[v_h-w]))$$
$$=p_{\text{spinon}}(v_h-w)\ . \tag{6.14}$$

At very low energies and near half-filling, the spinon-holon scattering phase shift is simply given by the momentum of the spinon p_{spinon}.

VII. THE SUPERSYMMETRY AND THE *t-J* MODEL

The *t-J* model in the form given by Sutherland [see (2.14)] shares some basic features characteristic of supersymmetric models.[36,37,60] However, an important distinction has to be made from ordinary supersymmetry theories:[61] the *t-J* Hamiltonian cannot be written as the sum of the squares of appropriate conserved charges. In the present model it is possible to place the holes (bosons) and the electrons (fermions) in a supermultiplet. Sutherland's Hamiltonian reads [see (2.14)]

$$H_S=\sum_{j=1}^{N_a}\mathcal{P}_{j,j+1}\ , \tag{7.1}$$

where $\mathcal{P}_{j,j+1}$ denotes a graded permutation operator. In fact, the Hamiltonian (7.1) can be directly diagonalized by means of a generalized QISM based on the graded counterpart of the Yang-Baxter algebra.[41]

Alternatively, the Hamiltonian (7.1) can be expressed in terms of the Hubbard operators where the occupancy of the lattice is restricted to at most one particle per site (we set $t=1$ in this section and define $X^{ab}=|a\rangle\langle b|$ with $a,b=0,\uparrow,\downarrow$) (Ref. 62)

$$H_S=\sum_{j,\sigma}(X_j^{0\sigma}X_{j+1}^{\sigma 0}+X_{j+1}^{0\sigma}X_j^{\sigma 0})$$
$$+\sum_{j,\sigma\sigma'}X_j^{\sigma\sigma'}X_{j+1}^{\sigma'\sigma}-\sum_j X_j^{00}X_{j+1}^{00}\ . \tag{7.2a}$$

The *t-J* Hamiltonian may be rewritten as

$$H_{tJ}=\sum_{j\sigma}(X_j^{0\sigma}X_{j+1}^{\sigma 0}+X_{j+1}^{0\sigma}X_j^{\sigma 0})$$
$$+\sum_{j\sigma}X_j^{\sigma-\sigma}X_{j+1}^{-\sigma\sigma}-\sum_{j\sigma}X_j^{\sigma\sigma}X_{j+1}^{-\sigma-\sigma}\ . \tag{7.2b}$$

The Hamiltonian (7.2a) is supplemented with the local constraint

$$X_i^{\uparrow\uparrow}+X_i^{\downarrow\downarrow}+X_i^{00}=1\ .$$

The Hubbard operators can be represented in terms of fermion fields as $X_j^{\sigma 0}=c_{j\sigma}^{\dagger}(1-n_{j-\sigma})$. Other explicit expressions may be obtained by applying the simple multiplication law $X_j^{ab}X_j^{cd}=\delta^{bc}X_j^{ad}$. For instance, the spin operators are linear in the X operators. The structure of the composition rules is

$$[X_i^{ab},X_j^{cd}]_{\pm}=\delta_{ij}(\delta^{bc}X_i^{ad}\pm\delta^{ad}X^{cb})\ , \tag{7.3}$$

where $[,]_{\pm}$ denotes a graded commutator, $[A,B]=AB-(-1)^{\alpha\beta}BA$, ($\alpha,\beta=0,1$ are the grades of A and B, respectively). The operators X^{ab} form a basis of the doubly graded superalgebra spl(1,2;C).[36] It is possible to construct a certain set of integrals of motion for H_S. We find that (for arbitrary dimension of the underlying lattice)[37,25]

$$[H_S,Q^{ab}]=0\ , \tag{7.4a}$$

where the conserved charges are defined as

$$Q^{ab}=\sum_j X_j^{ab},\quad \forall a,b=0,\uparrow,\downarrow\ . \tag{7.4b}$$

The supercharges Q^{ab} generate the same algebra as that defined by (7.3). Therefore the symmetry group of the Hamiltonian is the supergroup obtained by "exponentiation" of the superalgebra Spl(1,2;C) (see Ref. 61). The even part of the algebra, i.e., the subset $\{Q^{\sigma\sigma'},Q^{00}\}$ ($\sigma,\sigma'=\uparrow,\downarrow$), contains the algebra su(2). The odd part of the algebra is the set $\{Q_\sigma^{\pm}\}$ $\sigma=\uparrow,\downarrow$ [with the notation $Q_\sigma^{+}=Q^{\sigma 0}$, $Q_\sigma^{-}=(Q_\sigma^{+})^{\dagger}$]. Clearly, the supercharges $Q_\sigma^{\pm}$ are fermionic, i.e., $[Q_\sigma^s,Q_\sigma^s]_+=0$, $s=\pm$. As a consequence, the whole spectrum cannot be generated by successively applying the generators of the algebra. Notice that $Q_\sigma^z=[Q_\sigma^{+},Q_\sigma^{-}]_+=N_\sigma+N_h$ is also a (trivial) constant of motion. The supercharges $Q_\sigma^{\pm}$ connect in the Fock space the Hilbert spaces with different particle numbers, i.e., $[N,Q_\sigma^{\pm}]=\pm Q_\sigma^{+}$, and so are the supersymmetric analogs of the spin lowering (raising) operators. They annihilate (create) a particle with spin σ in a zero-momentum projected state: $Q_\sigma^{-}=\tilde{c}_{k=0\sigma}$, with $\tilde{c}_{k\sigma}=\mathcal{P}\sum_{j=1}^{N_a}e^{ikj}c_{j\sigma}\mathcal{P}$ ($\mathcal{P}$ is the projector defined in Sec. II).

From (7.4) it follows that

$$[H_{tJ},Q_\sigma^{\pm}]_-=\mp 2Q_\sigma^{\pm}\ . \tag{7.5}$$

The subset $\{Q_\sigma^{\pm},Q_\sigma^z\}$ (for each σ) generates a subalgebra

$$[Q_\sigma^z,Q_\sigma^{\pm}]_-=0\ , \tag{7.6a}$$
$$[Q_\sigma^{+},Q_\sigma^{-}]_+=Q_\sigma^z\ . \tag{7.6b}$$

At this point, it is interesting to remember the extra hidden SU(2) symmetry occurring in the Hubbard model. This particle-hole symmetry (which relates unoccupied and doubly occupied sites) is generated by a su(2) algebra

$$Q^{+}=(Q^{-})^{\dagger}=\sum_{j=1}^{N_a}(-1)^j c_{j\uparrow}^{\dagger}c_{j\downarrow}^{\dagger}\ , \tag{7.7a}$$
$$Q^z=\tfrac{1}{2}(N_a-N)\ . \tag{7.7b}$$

The Hubbard Hamiltonian H_{Hubbard}, in direct analogy with (7.5), obeys

$$[H_{\text{Hubbard}},Q^{\pm}]=\pm UQ^{\pm}\ , \tag{7.8}$$

where U denotes the Hubbard U. The symmetry algebra of the (modified) Hubbard Hamiltonian is (see, for example, Ref. 56) so(4)$\approx$su(2)$\otimes$su(2). In the same way, the subalgebra (7.6) characterizes in the *t-J* model the symmetry between the singly occupied and unoccupied sites. In the process of mapping the large-U Hubbard model to

the ($J \ll t$) t-J model, the extra SU(2) particle-hole symmetry is spoiled. However, the increase of J (so as to reach $2t=J$) restores a fermion-boson symmetry.

From (7.5) we infer that, to every eigenstate $|\Psi^N\rangle$ of H_{tJ} in the N-particle Hilbert space with energy E^N, there exist (with the proviso that $Q_\sigma^\pm|\Psi^N\rangle$ does not vanish) eigenstates of the $N\pm1$ and $N\pm2$-particle system given, respectively, by $|\Phi^{N\pm1}\rangle=Q_\sigma^\pm|\Psi^N\rangle$ and $|\Phi^{N\pm2}\rangle=Q_\sigma^\pm Q_{-\sigma}^\pm|\Psi^N\rangle$, and with energies $E^{N\pm1}=E^N\mp2$, $E^{N\pm2}=E^N\mp4$. The spin of these eigenstates follows from

$$[\mathbf{S}^2,Q_\sigma^\pm]=\tfrac{3}{2}Q_\sigma^\pm\mp\sigma Q_\sigma^\pm S^z\mp Q_{-\sigma}^\pm S^{-\sigma}\ , \tag{7.9a}$$

$$[S^z,Q_\sigma^\pm]=\pm\tfrac{1}{2}\sigma Q_\sigma^\pm\ , \tag{7.9b}$$

i.e., if $|\Psi^N\rangle$ is the singlet ground state then the state $|\Phi^{N\pm1}\rangle$ has spin $S=\frac{1}{2}$, $S^z=\sigma/2$. As a consequence the spectrum of the t-J model has a relatively simple structure as is observed in the numerical data obtained from exact diagonalization of small clusters.[42]

The commutation laws (7.3) imply a series of unusual relations (selection rules) between correlators defined in Hilbert spaces with different particle number. For instance, the spin-spin two-point function is easily shown to be such that

$$\langle\Psi'^{N-1}|S_i^zS_j^z|\Phi^{N-1}\rangle-\langle\Phi'^{N}|S_i^zS_j^z|\Psi^N\rangle$$
$$=(S_{\Psi'}^z-S_\Psi^z)\langle\Psi'^{N-1}|S_i^zX_j^{0\sigma}+X_i^{0\sigma}S_j^z|\Psi^N\rangle\ , \tag{7.10}$$

where it is assumed that $Q_\sigma|\Psi^N\rangle\neq0$ and that $|\Psi'^N\rangle$ is an excited state of the $N-1$-particle system (S_Ψ^z denotes the z component of the spin). Similar relations follow for the charge-charge correlator.[25]

It is instructive to note that if $|\Psi^{N_a}\rangle$ denotes the (singlet) ground state of the half-filled band then $Q_\sigma^\dagger|\Psi^{N_a}\rangle=0$ and $Q_\sigma|\Psi^{N_a}\rangle$ corresponds to a high-energy holon-spinon state (see Sec. VI). On the other hand, a two-particle eigenstate is constructed by applying successively $Q_\uparrow^\dagger$ and $Q_\downarrow^\dagger$ to the vacuum. It is a zero-momentum state (the ground state) with energy $E=-4$ and spin $S=S^z=0$. In this particular case, it is trivial that $Q_\sigma^\dagger|\Psi_0^2\rangle=0$ and $Q_\sigma|\Psi_0^2\rangle\neq0$. In fact, this is the generic case as can be seen from the numerical data.[42] This simply indicates that the ground state always contains zero momentum states. So far, our attempts to rigorously prove this statement have failed.

Finally, we emphasize that the supersymmetric properties of the model are independent of the dimension of the underlying lattice. They may be useful, for instance, in characterizing two-dimensional variational wave functions at the supersymmetric point.

VIII. CONCLUSION

In this work we have discussed the ground-state properties and excitation spectrum of the supersymmetric t-J model. We find that the Coulomb repulsion dominates the attractive exchange interaction. There are no real bound states in the problem and so no gap arises in the spectrum.

Recent numerical studies on the phase diagram of the t-J model[16] clearly indicate that the model belongs to the same universality class as that of the Hubbard model. Nevertheless, several new features emerge from our investigations. The holon-antiholon spectrum shows a $2k_F$ periodicity in momentum space, a fact which reflects the strong short-range AFM correlations. The spin spectrum reveals interesting properties. Near half-filling, the spin excitations behave as true spinons at low energies. In this region, the propagation of domain walls is essentially renormalized by the presence of holes. Doping a half-filled band with a few holes naturally leads to the separation of charge and spin degrees of freedom. As the filling decreases, the spin spectrum gradually transforms into a particle spectrum where charge and spin have recombined.

The numerical studies of Ref. 16 show clearly that the supersymmetric line is not a critical line and that phase separation occurs at higher values of the interaction with a dependence on the band filling. Moreover, the superconducting correlations dominate in a region which lies between the integrable line and the critical line.

Recently, Kawakami and Yang[20] have determined from finite-size analysis in conformal field theory the exponents of the large distance behavior of charge, spin, and superconducting correlation functions of the supersymmetric t-J model. They have shown that these exponents are those of the large-U Hubbard model near half-filling. In the dilute limit the exponents reduce to those of a noninteracting system. The analysis we propose of the excitation spectrum is consistent with these results. It illustrates the idea[50] that the separation of charge and spin degrees of freedom in the low energy spectrum is a universal feature of strongly correlated systems, and, as such, presumably a key concept in the understanding of the high-T_c materials.

ACKNOWLEDGMENTS

We are very much indebted to T. M. Rice for illuminating discussions, numerous suggestions, and crucial encouragement throughout the course of this work. We thank M. Luchini, W. Puttika, J. Rhyner, P. Schlottmann, and S. Sorella for helpful comments and correspondence. P.-A. Bares would like to thank N. Andrei, S. Barnes, B. Braun, S. Brazowsky, J. Carmelo, J.-P. Deredinger, G. Felder, R. Fernandez, J. Fröhlich, F. Guinea, F. D. M. Haldane, P. Horsch, M. Karowski, A. A. Ovchinnikov, R. Quadroni, M. Steiner, V. Telegdi, P. Wiegmann, and A. Zamolodchikov for stimulating discussions and encouragement. The support of the Swiss Nationalfonds is gratefully acknowledged.

APPENDIX A

In this appendix we briefly consider high energy excited states which are parametrized by real charge rapidities in Lai's formulation. As a function of band filling, they define a line which divides the spectrum into two sectors: excited states below the line necessarily involve complex roots in the charge rapidities whereas states above in-

volve only real charge rapidities. Although this type of excitation is irrelevant in discussing the low-energy physics of the model, it is instructive to carry out the calculations.

Consider Eqs. (2.11a) and (2.11b) and assume real roots for both the spin and charge rapidities. Taking the logarithm of (2.11) leads to

$$N_a 2\tan^{-1}(2v_j)=2\pi I_j+\sum_{\beta=1}^{M} 2\tan^{-1}(2[v_j-\Lambda_\beta]) , \quad \text{(A1)}$$

$$\sum_{j=1}^{N} 2\tan^{-1}(2[v_j-\Lambda_\alpha]) =2\pi J_\alpha+\sum_{\beta=1}^{M} 2\tan^{-1}(\Lambda_\beta-\Lambda_\alpha) , \quad \text{(A2)}$$

where the quantum numbers I_j are integers if N_a-M is even (h.o.i. otherwise) and J_α are integers if $N-M-1$ is even (h.o.i. otherwise). The energy and momentum are simply given by

$$E=-2t\sum_{j=1}^{N}\frac{4v_j^2-1}{4v_j^2-1} , \quad \text{(A3)}$$

$$P=\frac{2\pi}{N_a}\left[\sum_{j=1}^{N} I_j+\sum_{\alpha=1}^{M} J_\alpha\right] . \quad \text{(A4)}$$

In the thermodynamic limit we obtain the integral equations for the distribution of real roots

$$\rho(v)=\frac{1}{\pi}\frac{\frac{1}{2}}{(\frac{1}{2})^2+v^2} -\left[\int_{-\infty}^{-B}+\int_{B}^{\infty}\right]d\Lambda'\sigma(\Lambda')\frac{1}{\pi}\frac{\frac{1}{2}}{(\frac{1}{2})^2+(v-\Lambda')^2} , \quad \text{(A5)}$$

$$\sigma(\Lambda)=\left[\int_{-\infty}^{-Q}+\int_{Q}^{\infty}\right]dv\,\rho(v)\frac{1}{\pi}\frac{\frac{1}{2}}{(\frac{1}{2})^2+(v-\Lambda)^2} -\left[\int_{-\infty}^{-B}+\int_{B}^{\infty}\right]d\Lambda'\sigma(\Lambda')\frac{1}{\pi}\frac{1}{1+(\Lambda-\Lambda')^2} , \quad \text{(A6)}$$

where $\rho(v)$ and $\sigma(\Lambda)$ denote the distribution of charge and spin rapidities. Equations (A5) and (A6) have been solved numerically and the results are shown in Fig. 3. The nonanalyticity of the energy as a function of the band filling at $n=\frac{2}{3}$ (a point of high symmetry) can be seen as follows. Set $B=0$ in (A5) and (A6) and let Q vary on the interval $[0,\infty)$. $B=0$ implies that $M=N/2$ (N even) and so we are in the singlet sector. The energy in this case is given by

$$E=-2tN_a\left[n-\left[\int_{-\infty}^{-Q}+\int_{Q}^{\infty}\right]dv\,\rho(v)\frac{\frac{1}{2}}{(\frac{1}{2})^2+v^2}\right] . \quad \text{(A7)}$$

At $Q=0$ the band filling is $n=\frac{2}{3}$ whereas at $Q=\infty$ we obtain $n=0$. Therefore the singlet sector extends from $n=0$ to $n=\frac{2}{3}$ and the energy is analytic on the interval $[0,\frac{2}{3}]$.

Set now $Q=0$ and vary B. At $B=0$, $n=\frac{2}{3}$ (see above) and at $B=\infty$ we find $n=1$. Therefore at $Q=0$, the limit B alone determines the band filling. In this case, the integral equations (A5) and (A6) reduce to a single integral equation

$$\sigma(\Lambda)=\frac{1}{\pi}\frac{1}{1+\Lambda^2} -2\left[\int_{-\infty}^{-B}+\int_{B}^{\infty}\right]d\Lambda'\sigma(\Lambda')\frac{1}{\pi}\frac{1}{1+(\Lambda-\Lambda')^2} , \quad \text{(A8)}$$

or by using the Fourier transform technique

$$\sigma(\Lambda)=R_1(\Lambda)+2\int_{-B}^{B}d\Lambda'\sigma(\Lambda')R_1(\Lambda'-\Lambda) , \quad \text{(A9)}$$

where $R_1(x)$ denotes the function

$$R_1(x)=\frac{1}{2\pi}\int_{-\infty}^{\infty}dw\frac{e^{-i\omega x}}{e^{|\omega|}+2} . \quad \text{(A10)}$$

The energy can be written as

$$E=-tN_a\{1-\pi\sigma(0)\} . \quad \text{(A11)}$$

Notice that the energy is an analytic function of n on the interval $[\frac{2}{3},1]$ and that the reality of the roots enforces the state to acquire a finite magnetization as is easily seen from the fact that B is finite.

APPENDIX B

In this appendix we wish to discuss briefly a technical problem which arises when dealing with the two-string ansatz (3.1). The ansatz in the form (3.1) applies only in the thermodynamic limit and is consistent with a detailed analysis of the BAE of the Gross-Neveu model performed by Destri and Lowenstein.[63] As emphasized in Sec. III, in writing Eq. (3.3c) it was implicitly assumed that the ansatz (3.1) remains valid for all values of the real part v_α. There is however a pair of roots of (2.11) which lies outside the ansatz (3.1) namely, when the real part tends to infinity so does the imaginary part. For a finite system these pairs of roots must be factored out explicitly. The correct thermodynamic limit can then be performed. A careful treatment of this limit yields[25]

$$N_a\theta(v_\alpha)=2\pi I_\alpha+\sum_{\beta=1}^{N/2-1}\theta(v_\alpha-v_\beta) , \quad \text{(B1)}$$

where the quantum numbers I_α are now integers if (N_a-M) is even and h.o.i. otherwise. They are restricted to the interval (3.4) but with $I_{\max}=(N_a-M)/2-1$. In the thermodynamic limit either (3.3c) or (B1) lead to the same result for the energy. However the expression for the crystal momentum obtained from (3.3c) is erroneous (compare with the results of Sec. V). For example, in the case of a nondegenerate ground state, i.e., N_a even and $N/2$ odd, the crystal momentum which follows from (B1) is zero whereas (3.3c) yields a finite momentum in contradiction with the results obtained from exact diagonalization of small clusters. It is worth noting that the number of pairs of complex conjugate roots of Eq. (3.3d) is exactly equal to the number of roots of Eq. (B1). For

the purposes of investigating the properties of a macroscopic system it is more convenient to work with (3.3c) rather than (B1): the singular roots of (2.11) need not be treated separately. This approach is legitimate as long as we remember that only the relative momenta are reproduced correctly by (3.3c). In this paper we do so when dealing with the excitation spectrum in Lai's formulation. It can be shown in a careful treatment of the BAE[25] that all the results derived in this work are correct for the energies and relative momenta. Moreover the results of Secs. III and IV are reproduced using Sutherland's representation where no such difficulties arise: we find perfect agreement. Nonetheless, we wish to emphasize that for a finite system, the singular roots of (2.11) may be at the origin of difficulties in a straightforward numerical approach.

Clearly Eqs. (3.3a) and (3.3c) are not equivalent to (2.11) for a finite system: (3.3a) may be obtained from (2.11) by substituting the ansatz (3.1) and taking the ratio of two complex conjugate expressions in order to cancel a divergence arising in the thermodynamic limit. For a finite system this last operation eventually cancels a factor (-1) and hence (3.3a) has more solutions in this sector than (2.11). Despite this fact, (3.3c) gives the correct energetics: the reason is that in the thermodynamic limit the roots of (3.3a) become degenerate with those which one would obtain for the real part of the two-strings in (2.11) (except for the singular roots discussed above). Therefore, for the purposes of studying systems of finite size, one should start with (2.11) or (2.13).

APPENDIX C

In this appendix we wish to mention a representation of the t-J model in terms of the generators of a spin $S=1$ su(2) algebra. The original motivation for seeking such a representation was its convenience to numerical studies at arbitrary values of the interaction and its eventual generalization to 2D. This representation shows that the model is not SU(3) invariant at the supersymmetric point. We restrict our considerations here to the case $2t=J$.[25]

From the definition of the Hubbard operators, it follows that at any given site j they obey a $u(3)$ algebra. However, operators at different sites commute or anticommute according to their grades. The idea is to extend the $u(3)$ algebra to the case when the X operators act on different sites. In order to do this we introduce two types of hard core fermions: $Y_j^{0+}=X_j^{0\uparrow}$ and $Y_u^{0-}=X_j^{0\downarrow}\prod_{l=1}^{N_a}(2X_{ll}^{\uparrow\uparrow}-1)$. This transformation leaves the Hamiltonian (7.2a) [and (7.2b)] invariant and alters the commutation rules (7.3). For each $s=\pm$, the Y operators obey (7.3), i.e., $[Y_j^{0s},Y_i^{0s}]_+=\delta^{ji}(Y_i^{00}+Y_i^{ss})$, whereas for different s the usual commutator should be taken in (7.3), i.e., $[Y_j^{0s},Y_i^{0-s}]_-=0$. It is now possible to transform the Y_i operators to a new set of variables A_i which obey a u(3) algebra:

$$[A_j^{ab},A_i^{cd}]_-=\delta^{ji}(\delta^{bc}A_j^{ad}-\delta^{ad}A_j^{cb})\ . \tag{C1}$$

This is achieved by means of a Jordan-Wigner transformation for $s=\pm$

$$A_j^{s0}=Y_j^{s0}e^{i\pi\sum_{l=1}^{j-1}Y_l^{ss}}\ . \tag{C2}$$

In terms of the new variables, the t-J Hamiltonian reads

$$\begin{aligned}H_{tJ}=&\sum_{j=1s=\pm}^{N_a}(A_j^{0s}A_{j+1}^{s0}+A_{j+1}^{0s}A_j^{s0})\\&-\sum_{j=1s=\pm}^{N_a}A_j^{s-s}A_{j+1}^{-ss}-\sum_{j=1s=\pm}^{N_a}A_j^{ss}A_{j+1}^{-s-s}\\&+\sum_{s=\pm}(A_{N_a}^{0s}A_1^{s0}+A_1^{0s}A_{N_a}^{s0})(1+e^{i\pi\mathcal{N}^a})\\&+(1-e^{i\pi\mathcal{N}})\sum_{s=\pm}A_{N_a}^{s-s}A_1^{-ss}\ ,\end{aligned} \tag{C3}$$

where $\mathcal{N}^s=\sum_{j=1}^{N_a}A_j^{ss}$ and $\mathcal{N}=\mathcal{N}^+ +\mathcal{N}^-$. The last two terms in (C3) arise from the cyclic boundary conditions and may be neglected for a large system. The form of the local constraint on the X operators remains unaltered by these transformations: $A_i^{++}+A_i^{--}+A_i^{00}=1$. We define spin operators according to

$$S_i^+=\sqrt{2}(A_i^{+0}+A_i^{0-})=[S_i^-]^\dagger\ , \tag{C4a}$$

$$S_i^z=A_i^{++}-A_i^{--}\ . \tag{C4b}$$

It is easy to verify that the spin operators defined in (C4) generate a spin $S=1$ representation of SU(2). On account of (7.14) and omitting boundary terms in (C4), the t-J Hamiltonian can be written as

$$\begin{aligned}H_{tJ}=&2\sum_{i=1}^{N_a}(1-[S_i^z]^2)-\sum_{i=1}^{N_a}(\mathbf{S}_i\cdot\mathbf{S}_{i+1}+[\mathbf{S}_i\cdot\mathbf{S}_{i+1}]^2)\\&+\sum_{i=1}^{N_a}(S_i^zS_{i+1}^z+[S_i^zS_{i+1}^z]^2)\ .\end{aligned} \tag{C5}$$

Alternatively, the pseudospin Hamiltonian (C5) may be obtained using a slave boson approach.[64] The constants of motion (7.5) have no longer a simple expression in terms of the spin operators and their interpretation in these variables is complicated by the fact that the symmetry mixes states of different spin. Notice that the band filling in the original Hamiltonian fixes the magnitude of $\sum_i[S_i^z]^2$.

[1]P. W. Anderson, Science **235**, 1196 (1987).
[2]F. C. Zhang and T. M. Rice, Phys. Rev. B **37**, 3759 (1988).
[3]E. H. Lieb and F. Y. Wu, Phys. Rev. Lett. **20**, 1445 (1968).
[4]W. Kohn, Phys. Rev. **133**, A171 (1964); A. B. Harris and R. V. Lange, Phys. Rev. **157**, 295 (1967); W. F. Brinkman and T. M. Rice, Phys. Rev. B **2**, 1324 (1970); C. Castellani, C. di Castro, and D. Feinberg, Phys. Rev. Lett. **43**, 1957 (1979); J. E. Hirsch, *ibid.* **54**, 1317 (1985); C. Gros, R. Joynt, and T. M. Rice, Phys. Rev. B **36**, 386 (1986).
[5]P. W. Anderson, Phys. Rev. Lett. **65**, 2306 (1990).
[6]C. K. Lai, J. Math. Phys. **15**, 1675 (1974).
[7]B. Sutherland, Phys. Rev. B **12**, 3795 (1975).
[8]P. Schlottmann, Phys. Rev. B **36**, 5177 (1987).
[9]P.-A. Bares, in Proceedings of Third European Conference on

Low Dimensional Conductors and Superconductors, Dubrovnik, Yugoslavia, 1989 [Fizika **21** (S3), 67 (1989)].
[10]P.-A. Bares and G. Blatter, Phys. Rev. Lett. **64**, 2567 (1990).
[11]P.-A. Bares is indebted to N. Andrei for drawing to his attention the work of S. Sarkar.
[12]S. Sarkar, J. Phys. A **23**, L409 (1990).
[13]M. Imada and Y. Hatsugai, J. Phys. Soc. Jpn. **58**, 3752 (1989).
[14]K. J. von Szcepanski, P. Horsch, W. Stephen, and M. Ziegler, Phys. Rev. B **41**, 2017 (1990).
[15]F. F. Assaad, and D. Würtz, Phys. Rev. B (to be published).
[16]M. Ogata, M. U. Luchini, S. Sorella, and F. F. Assaad, Phys. Rev. Lett. **66**, 2388 (1991).
[17]F. D. M. Haldane, J. Phys. C **14**, 2585 (1981).
[18]F. Woynarowich, J. Phys. A **22**, 4243 (1989).
[19]H. Frahm and V. E. Korepin, Phys. Rev. B **43**, 5653 (1991).
[20]N. Kawakami and S.-K. Yang, Phys. Rev. Lett. **65**, 2309 (1990).
[21]J. Carmelo and A. A. Ovchinnikov, J. Phys.: Condens. Matter **3**, 757 (1991).
[22]J. Carmelo, P. Horsch, P.-A. Bares, and A. A. Ovchinnikov, Int. J. Mod. Phys. B **5**, 3 (1991).
[23]J. Carmelo, P.-A. Bares, and P. Horsch (unpublished).
[24]J. Carmelo and P.-A. Bares (unpublished).
[25]P.-A. Bares, Ph.D. thesis at the ETH-Zürich, (1991).
[26]C. N. Yang, Phys. Rev. Lett. **19**, 1312 (1967).
[27]M. Gaudin, in *La Fonction d'Onde de Bethe* (Collection du Commissariat à l'Energie Atomique, Edition Masson, 1983).
[28]R. J. Baxter, *Exactly Solved Models in Statistical Mechanic* (Academic, London, 1989).
[29]L. A. Takhtajan, in *Exactly Solvable Problems in Condensed Matter and Relativistic Field Theory,* edited by B. S. Shastry *et al.* (Springer-Verlag, Berlin, 1985), p. 175.
[30]A. M. Tsvelick and P. B. Wiegmann, Adv. Phys. **32**, 453 (1983).
[31]H. B. Thacker, Rev. Mod. Phys. **53**, 253 (1981).
[32]The original idea goes back to H. Bethe (Ref. 34).
[33]Other boundary conditions consistent with the Bethe ansatz can be used, for instance twisted boundary conditions; see B. S. Shastry and B. Sutherland, Phys. Rev. Lett. **65**, 243 (1990); M. J. Martins and R. M. Fye (unpublished).
[34]H. Bethe, Z. Phys. **71**, 205 (1931).
[35]B. Sutherland, in *Exactly Solvable Problems in Condensed Matter and Relativistic Field Theory* (Ref. 29), p. 1.
[36]P. B. Wiegmann, Phys. Rev. Lett. **60**, 821 (1988).
[37]D. Foerster, Phys. Rev. Lett. **63**, 2140 (1989).
[38]This simply follows from the fact that $H(t,-J) = -H(-t,J)$.
[39]The case of two particles does not require these consistency conditions and is easily solved for all values of g. Above the supersymmetric point, the ground state is a two-particle bound state.
[40]As pointed out by Sutherland (Ref. 7), Lai's solution is correct for the case $\Delta=1$ (here $2t=J$), whereas it is in error for $\Delta=-1$ (here $2t=-J$). The BAE of Ref. 8 must be corrected as follows: in the AFM case one should read $p=\frac{1}{2}\cot(k/2)$ whereas in the FM case $p=\frac{1}{2}\tan(k/2)$.
[41]P. P. Kulish and E. K. Sklyanin, J. Sov. Math. **19**, 1596 (1982).
[42]M. Ogata (unpublished).
[43]L. Hulthen, Ark. Mat. Astron. Fys. Bd **26A**, 1 (1938).
[44]H. Shiba, Phys. Rev. B **6**, 930 (1972).
[45]H. Schultz, Phys. Rev. Lett. **64**, 2831 (1990).
[46]N. M. Bogoliubov, A. G. Izergin, and V. E. Korepin, Nucl. Phys. **B275**, [FS17], 687 (1986).
[47]V. E. Korepin, Teor. Mat. Fiz. **41**, 169 (1979).
[48]F. Woynarowich, J. Phys. C **16**, 6593 (1983).
[49]C. F. Coll, Phys. Rev. B **9**, 2150 (1974).
[50]P. W. Anderson, Int. J. Mod. Phys. B **4**, 181 (1990).
[51]L. D. Faddeev and L. A. Takhtajan, Phys. Lett. **85A**, 375 (1981).
[52]S. I. Matveenko, Zh. Eksp. Teor. Fiz. **94**, 213 (1988) [Sov. Phys. JETP **7**, 1416 (1988)].
[53]The thermodynamics of the model has been investigated by Schlottmann in Lai's representation (Ref. 8) and can be reformulated in Sutherland's representation (Ref. 25).
[54]H. J. Schultz, Int. J. Mod. Phys. B **5**, 57 (1991).
[55]A single hole in a zero-momentum state can be inserted by applying the supercharge Q_σ^- (see Sec. VII) to the ground state of the half-filled band. The energy and crystal momentum of the one-hole doped system obtained in this way are given, respectively, by $E=2tN_a\ln 2+2t$, and $p=0$.
[56]F. D. M. Haldane and Y. Tu (unpublished).
[57]G. Gómez-Santos, Phys. Rev. B **41**, 6788 (1990).
[58]In Lai's representation the additional branches at $\pm 2k_F$ are characterized by the presence of a pair of rapidities on the real axis.
[59]X. Zotos, P. Prelovsek, and I. Sega, Phys. Rev. B **42**, 8445 (1990).
[60]A. V. Markelov (unpublished).
[61]See, for example, P. G. O. Freund, *Supersymmetry* (Cambridge University Press, England, 1986).
[62]A representation of the t-J Hamiltonian in terms of spin $S=1$ operators is derived in Appendix C.
[63]C. Destri and J. H. Lowenstein, Nucl. Phys. **B205**, [FS5], 369 (1982).
[64]T. Barnes (private communication).